3 RESULTS AND DISCUSSION

3.1 Syntheses of ligand and complexes

The 2-(phenylazo)pyrazine (azine) ligand was obtained by the condensation of the 2-(phenylazo)pyrazine and the nitrosobenzene in 1:1 mole ratio in sodium hydroxide and benzene. The red-orange product was isolated from this reaction mixture by column chromatography. The reaction are shown in equation (1).

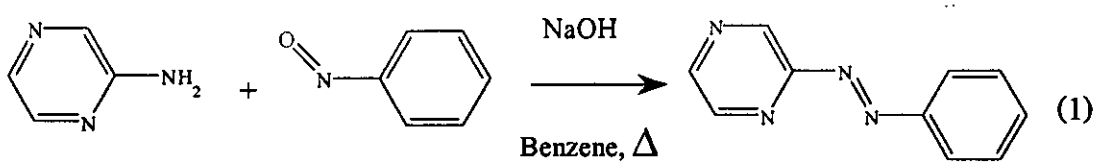

(1)

2-aminopyrazine nitrosobenzene 2-(phenylazo)pyrazine (azine)

The yield obtained was 52 %. The physical properties of the azine ligand are summarized in table 1.

Table 1. The physical properties of azine

Ligand	Physical properties		
	Appearance	Color	Melting point (°C)
azine	Solid	Red-orange	66-68

The melting point of the azine ligand was in the range 66-68 °C. The red-orange ligand was in solid state at room temperature. The solubility of 10 mg of ligand

was tested in 5 mL of various solvents. The ligand was very soluble in almost all solvents, but slightly soluble in water.

In the present work, the ruthenium complexes with the 2-(phenylazo)pyrazine (azine) ligand were prepared from $RuCl_3.3H_2O$ and the azine ligands in boiling DMF or 1-propanol. The reactions afford the three isomers. There were *ctc*, *ccc* and *tcc*-[Ru (azine)$_2$Cl$_2$] complexes. The coordination number of these complexes were six and the two azine ligands acted as a bidentate ligand. The physical properties of the complexes are summarized in table 2.

Table 2. The physical properties of the [Ru(azine)$_2$Cl$_2$] complexes

Ligand	Physical properties		
	Appearance	Color	Melting point (°C)
ctc-[Ru(azine)$_2$Cl$_2$]	Solid	Dark blue	228-230
ccc-[Ru(azine)$_2$Cl$_2$]	Solid	Blue	250-252
tcc-[Ru(azine)$_2$Cl$_2$]	Solid	Green	296-298

The solubilities of 10 mg of the [Ru(azine)$_2$Cl$_2$] complexes were tested in 5 mL of various solvents. The complexes were soluble in MeOH, EtOH, toluene, and more soluble in acetone. It was completely soluble in dichloromethane, chloroform and acetonitrile solvents but insoluble in hexane, ether, and water.

3.2 Characterization of ligand and complexes

The chemistries of the azine ligand and their complexes were determined by using these techniques

3.2.1 Elemental analysis

3.2.2 Fast-atom bombardment (FAB) mass spectrometry

3.2.3 Infrared spectroscopy

3.2.4 UV-Visible absorption spectroscopy

3.2.5 Nuclear Magnetic Resonance spectroscopy (1D and 2D)

3.2.6 Cyclic Voltammetry

3.2.7 X-ray Crystallography

3.2.1 Elemental analysis

Elemental analysis is a technique to study composition of elements in a compound. It is shown that, the analytical data of the compound corresponded to the calculated values.

The elemental analysis data are listed in Table 3.

Table 3. Elemental analysis data of the azine ligand and the $[Ru(azine)_2Cl_2]$ complexes

Ligand	% C		% H		% N	
	Calc.	Found	Calc.	Found	Calc.	Found
azine	65.22	65.35	4.38	4.38	30.42	30.32
ctc-$[Ru(azine)_2Cl_2]$	44.45	44.49	2.98	3.03	20.74	20.76
ccc-$[Ru(azine)_2Cl_2]$	44.45	42.56	2.98	2.83	20.74	19.71
tcc-$[Ru(azine)_2Cl_2]$	44.45	44.08	2.98	2.84	20.74	21.18

3.2.2 Fast-atom bombardment (FAB) mass spectrometry

The FAB mass spectrometry is a technique to study molecular mass of compound.

The FAB mass spectrum of the azine ligand is shown in Figure 4. From the data, the maximum peak, which gave 100% relative abundance at m/z 185 corresponded to the molecular weight of azine with one proton.

The *ctc*-[Ru(azine)$_2$Cl$_2$] complex showed the most intense peak at m/z 505, which was assigned to *ctc*-[Ru(azine)$_2$Cl]$^+$ (90%). The FAB mass spectra are shown in Figure 5.

The parent peak of the *tcc*-[Ru(azine)$_2$Cl$_2$] complex gave 100% relative abundance at m/z 57 ,which were assigned to $CH_3(CH_2)_2OH$ solvent. The FAB mass spectra are displayed in Figure 7.

This method could confirm the formula and molecular mass of the ligand and the complexes as expected. The results from this technique are summarized in the Table 4.

Table 4. FAB mass spectroscopic data of azine and [Ru(azine)$_2$Cl$_2$]

Compounds	m/z	Stoichiometry	Equivalent species	Rel. Abun. (%)
azine	185	[azine+H]$^+$	[L+H]$^+$	100
ctc-[Ru(azine)$_2$Cl$_2$]	505	[M-Cl]	[M-Cl]	90
tcc-[Ru(azine)$_2$Cl$_2$]	57	$CH_3(CH_2)_2OH$	$CH_3(CH_2)_2OH$	100

MW. of azine (L) = 184.20 g/mol, MW. of [Ru(azine)$_2$Cl$_2$] (M) = 540.37 g/mol

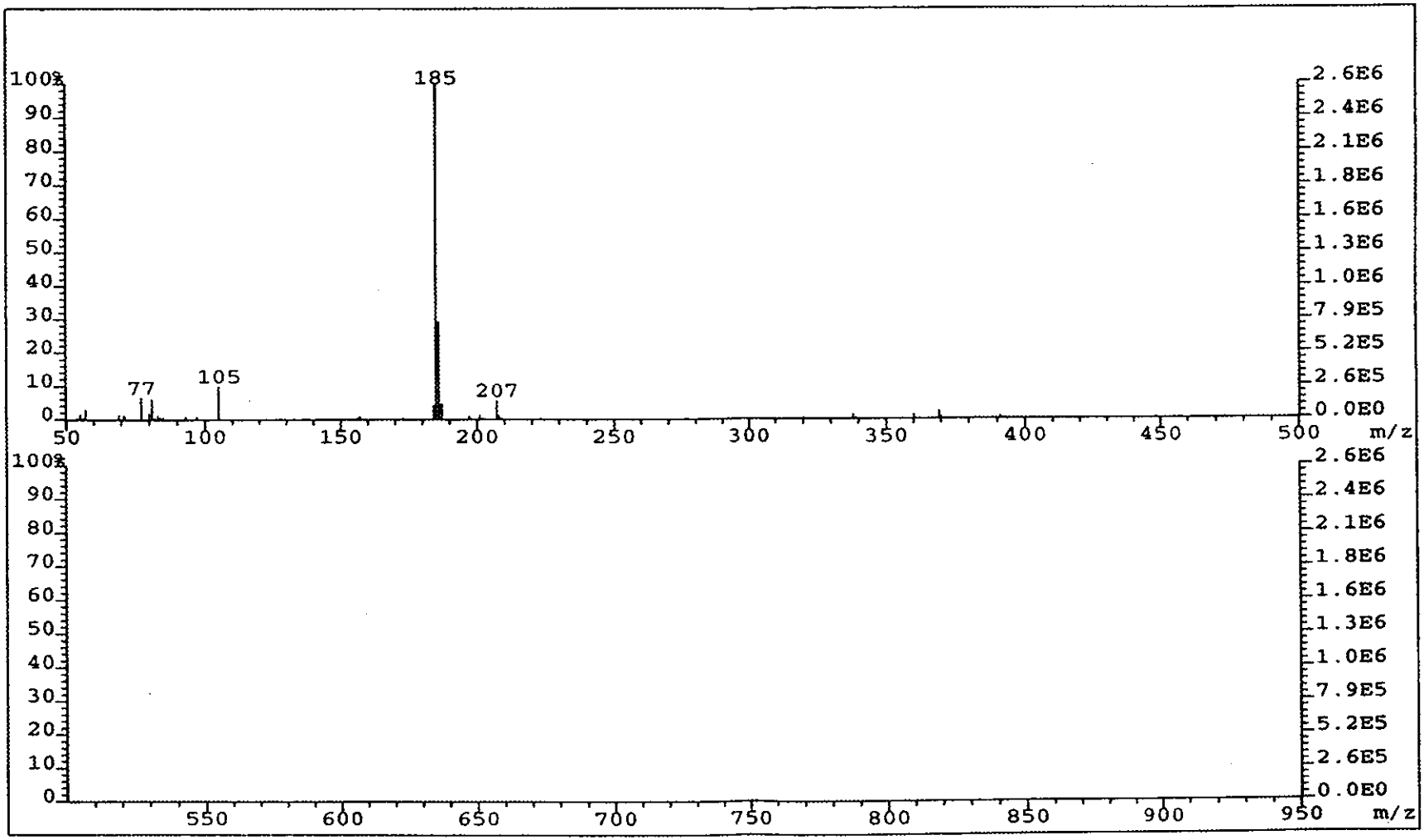

Figure 4. FAB mass spectrum of azine.

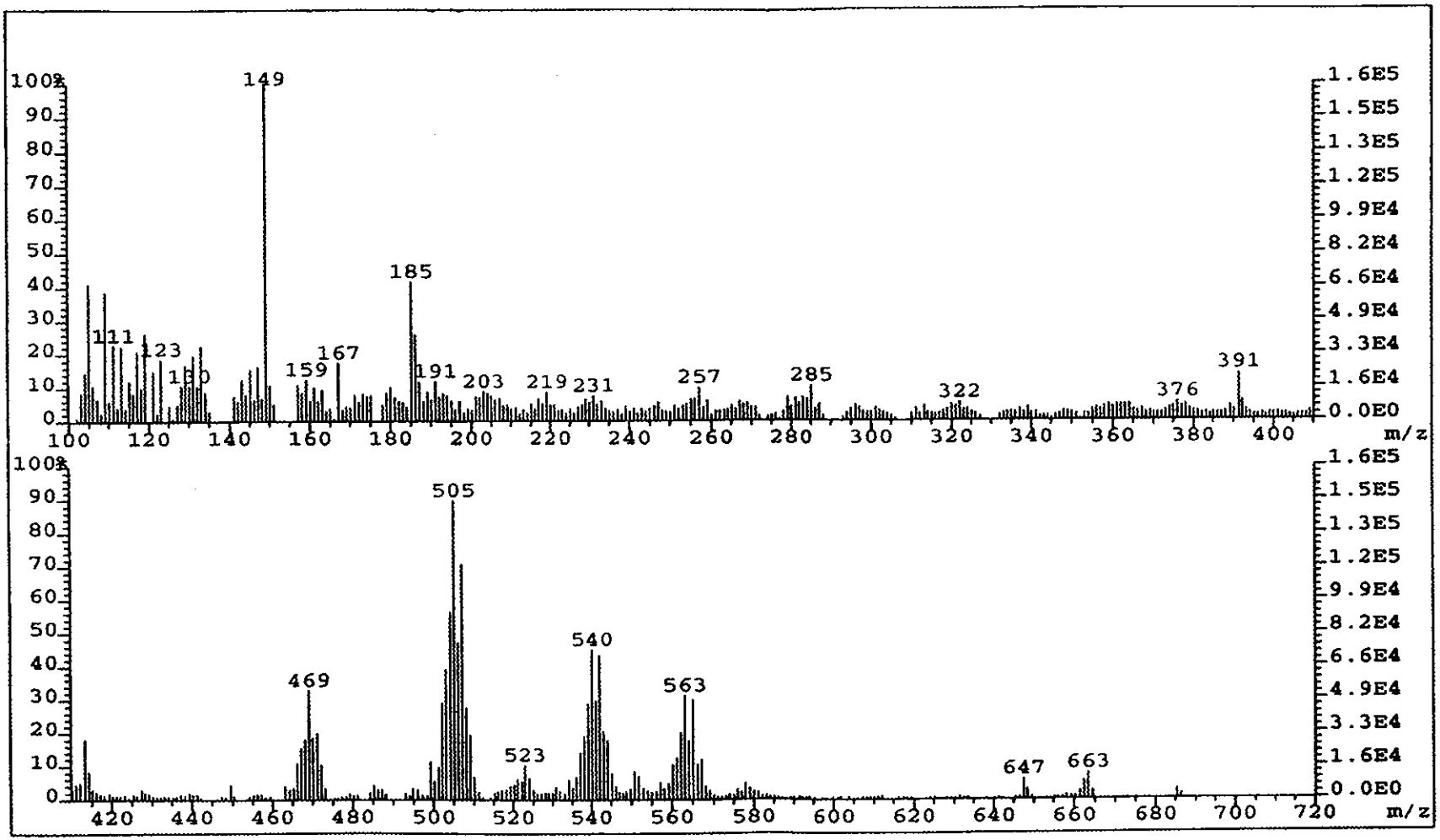

Figure 5. FAB mass spectrum of *ctc*-[Ru(azine)$_2$Cl$_2$].

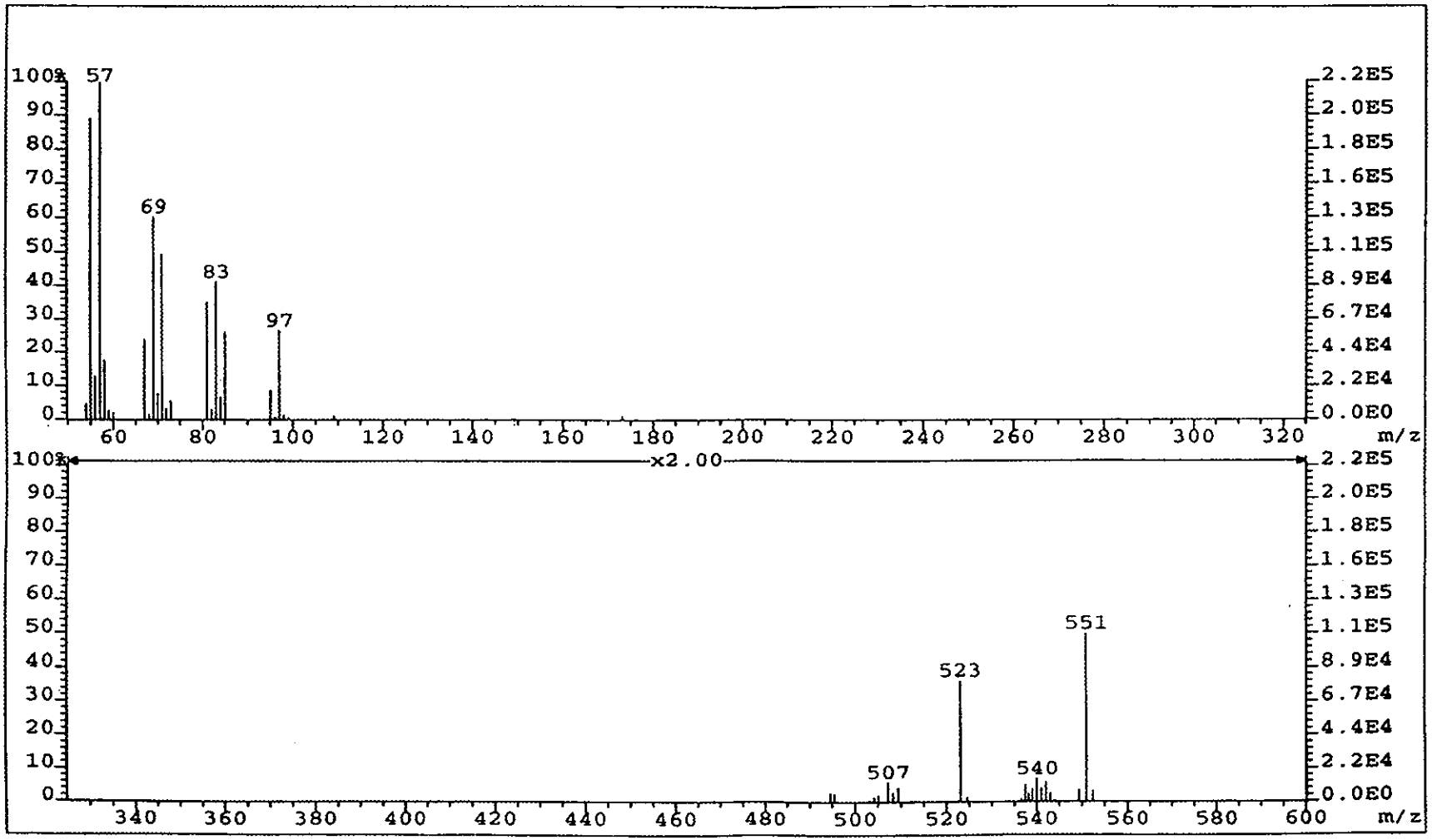

Figure 6. FAB mass spectrum of *tcc*-[Ru(azine)$_2$Cl$_2$].

3.2.3 Infrared spectroscopy

Infrared spectroscopy is a technique to study the functional groups of compounds. Infrared spectra were collected by using KBr pellets in the range 4000-370 cm^{-1}. The important vibrational frequencies are C=C, C=N, N=N (azo) stretching modes and C-H bending in monosubstituted benzene.

Infrared spectroscopy of the azine ligand

The infrared spectroscopic data of the azine ligand are listed in Table 5.

Table 5. Infrared spectroscopic data of the azine ligand

Vibration modes	Frequencies (cm^{-1})
C=C, C=N stretching	1583 (m) 1465 (m) 1435 (m) 1428 (m)
N=N stretching	1388 (m)
C-H bending in monosubstituted benzene	779 (s) 742 (s) 687 (s)

s = strong, m = medium

The infrared spectrum of azine exhibited several intense vibrational bands in the range 1600-370 cm^{-1}. Four medium peaks observed in the range 1583-1428 cm^{-1} were corresponded with the C=C and C=N stretching in the pyrazine ring of ligand. The

most important peak was the N=N stretching mode which was used to be considered the π-acid property in azo complexes. The N=N stretching mode displayed a strong peak at 1388 cm^{-1}, which was lower frequency than that in azpy (1421 cm^{-1}) (Changsaluk, U., 2003). While, the azpym ligand provided the peak at 1392 cm^{-1} (Rattanawit, N., 2002). These results indicated that the N=N bond of the free azpy ligand is stronger than those of azpym and azine ligands. In addition, this vibrational band is expected to be higher frequency than that in the complexes. The infrared spectrum is shown in Figure 8.

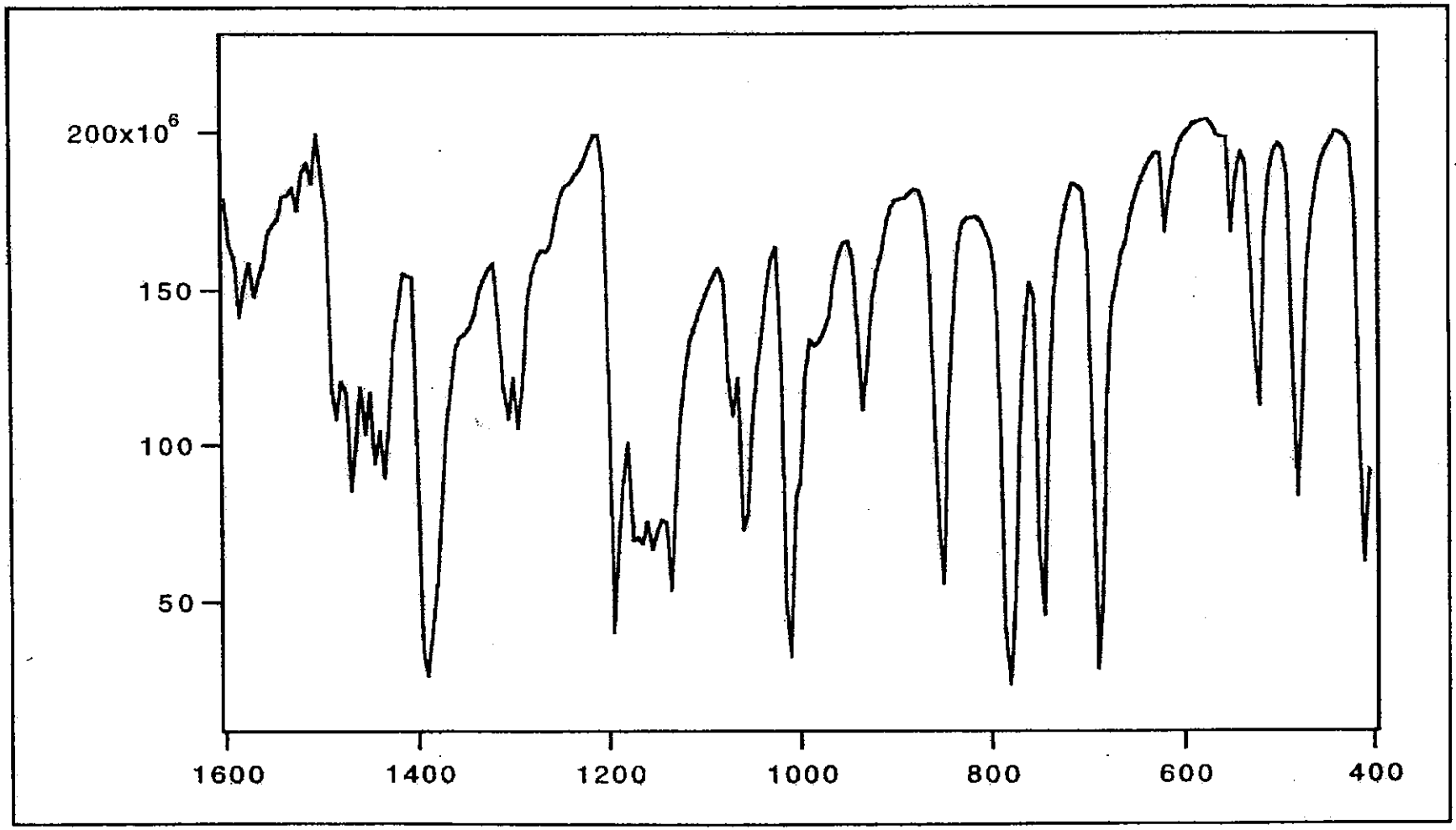

Figure 7. IR spectrum of azine.

Infrared spectroscopy of the $[Ru(azine)_2Cl_2]$ complexes

The infrared spectroscopic data of the complexes are listed in Table 6.

Table 6. Infrared spectroscopic data of $[Ru(azine)_2Cl_2]$

Vibration modes	Frequencies (cm^{-1})		
	ctc-$[Ru(azine)_2Cl_2]$	*ccc*-$[Ru(azine)_2Cl_2]$	*tcc*-$[Ru(azine)_2Cl_2]$
C=C, C=N stretching	1579 (m)	1576 (m)	1584 (m)
	1472 (m)	1490 (m)	1480 (m)
	1443 (m)	1443 (m)	1450 (m)
	1413 (m)	1413 (m)	1410 (m)
N=N stretching	1310 (s)	1303 (s)	1297 (s)
C-H bending in monosubstituted benzene	772 (m)	768 (m)	751 (m)
	760 (m)	705 (m)	705 (m)
	731 (m)	683 (m)	687 (m)

s = strong, m = medium

Infrared spectra of the three complexes displayed four medium peaks at 1584-1410 cm^{-1}. These frequencies were assigned to the C=C and the C=N vibrational modes. The strong peak observed in the range 1310-1297 cm^{-1} corresponded to the N=N stretching mode and these were red shifted by 80-90 cm^{-1} compared to the free ligand value (1388 cm^{-1}). While, the ν(N=N) in the azpym complexes were red shifted by 25-30 cm^{-1} (Santra, *et al.*,1999). The N=N stretching frequencies of the ligand and the complexes are summarized in Table 7.

Table 7. The N=N stretching frequencies of the ligand and the complexes

Compounds	N=N stretching (cm^{-1})
azine	1388
ctc-[Ru(azine)$_2$Cl$_2$]	1310
ccc-[Ru(azine)$_2$Cl$_2$]	1303
tcc-[Ru(azine)$_2$Cl$_2$]	1297

The N=N stretching modes in the complexes appeared at lower frequency than that in the free ligand. It was due to the π-back bonding occurring from the t_{2g} orbitals of metal to the π^* orbitals of azo. Then the bond order of N=N (azo) decreased and the vibrational energies decreased. Furthermore, ν(N=N) of the ctc isomer appeared at the higher frequency than the ccc and the tcc isomers. It indicated that the azine in ctc could accept electrons from the t_{2g} orbitals to its π^* orbitals less than ccc and tcc (tcc > ccc > ctc). The infrared spectra of the [Ru(azine)$_2$Cl$_2$] isomers are shown in Figure 9, 10 and 11, respectively.

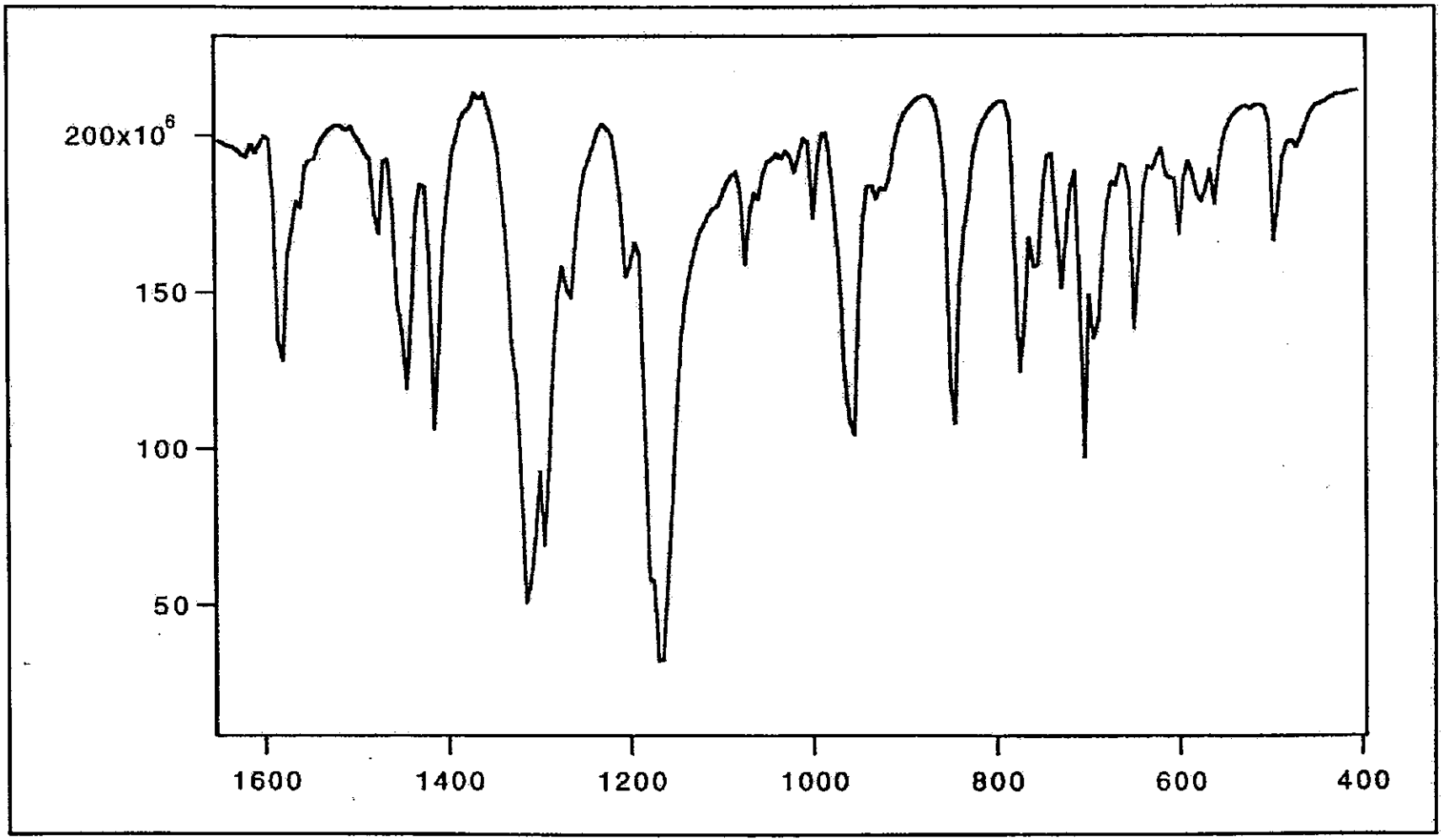

Figure 8. IR spectrum of *ctc*-[Ru(azine)$_2$Cl$_2$].

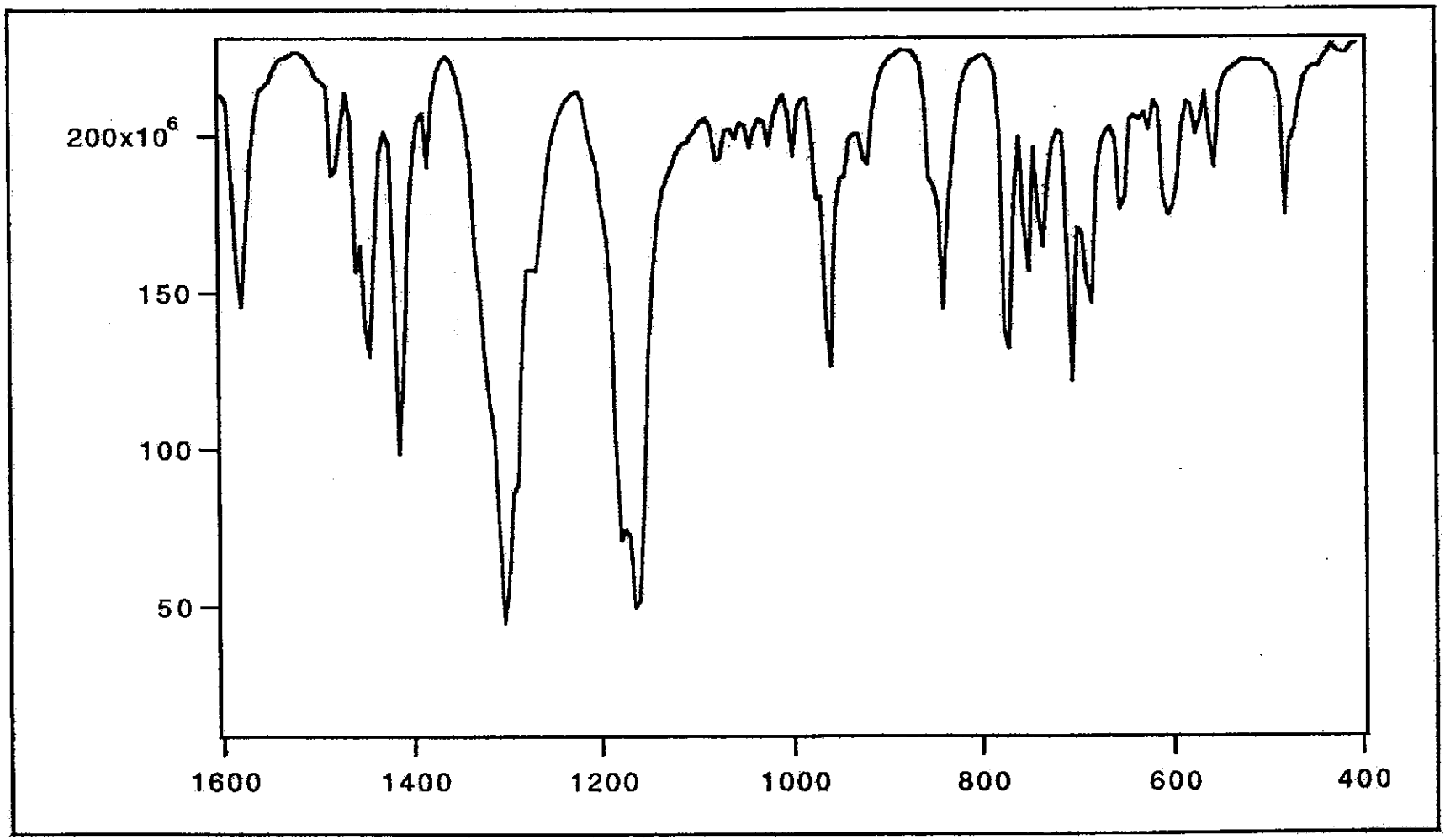

Figure 9. IR spectrum of *ccc*-[Ru(azine)$_2$Cl$_2$].

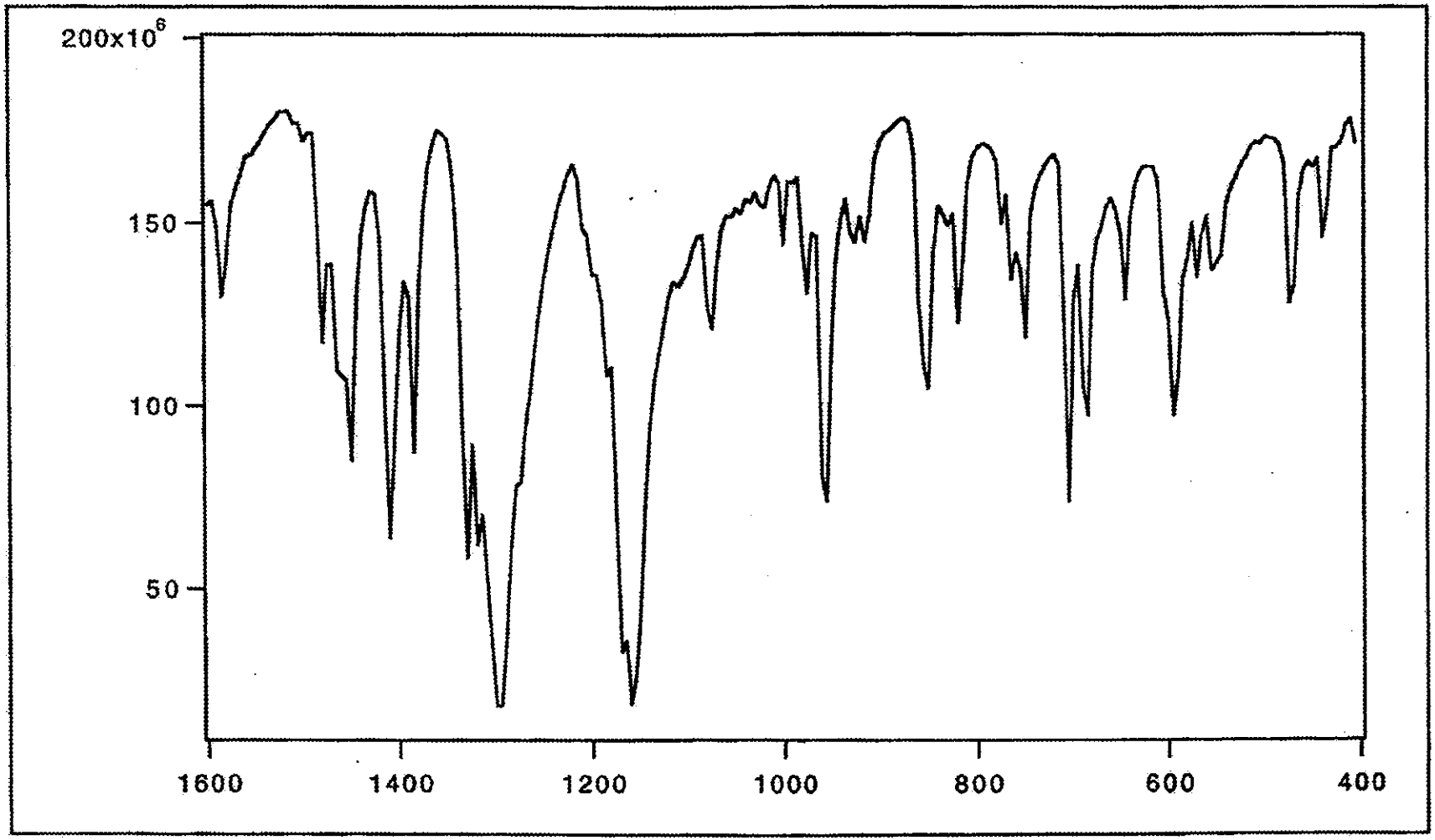

Figure 10. IR spectrum of *tcc*-[Ru(azine)$_2$Cl$_2$].

3.2.4 UV-Visible absorption spectroscopy

UV-Visible absorption spectroscopy is a technique to study the electronic transitions of compound. The electronic absorption spectral data were measured from 200 nm to 800 nm in CH_2Cl_2, $CHCl_3$, CH_3CN, DMF and DMSO. The spectral data are listed in Table 8.

Table 8. UV-Visible absorption spectroscopic data of the ligand and the complexes

compounds	λ_{max} nm, ($\varepsilon^a \times 10^{-4}$ $M^{-1}cm^{-1}$)				
	CH_2Cl_2	$CHCl_3$	CH_3CN	DMF	DMSO
azine	321 (1.9)	324 (1.9)	316 (1.8)	319 (1.7)	321 (1.7)
	462 (0.05)	459 (0.03)	458 (0.02)	455 (0.04)	454 (0.05)
ctc - $[Ru(azine)_2Cl_2]$	338 (2.8)	339 (2.7)	334 (2.7)	338 (3.0)	339 (2.8)
	580 (1.1)	582 (1.1)	578 (1.1)	583 (1.2)	583 (1.1)
ccc - $[Ru(azine)_2Cl_2]$	361 (2.0)	364 (1.8)	348 (1.8)	350 (1.8)	353 (2.0)
	582 (0.5)	584 (0.9)	576 (0.9)	581 (0.8)	579 (1.0)
tcc - $[Ru(azine)_2Cl_2]$	437 (1.2)	440 (1.2)	428 (1.1)	428 (1.1)	431 (1.2)
	657 (1.1)	657 (1.1)	646 (1.0)	660 (1.0)	660 (1.1)

[a] Molar extinction coefficient

UV-visible spectral studies of the free ligand revealed absorption at 316-324 nm ($\varepsilon \approx 18000$ $M^{-1}cm^{-1}$) and 454-462 nm ($\varepsilon \approx 400$ $M^{-1}cm^{-1}$), which were due to intraligand charge transitions, $\pi \rightarrow \pi^*$ and $n \rightarrow \pi^*$, respectively. Figure 12 shows the UV-Visible absorption spectrum for the azine ligand in CH_3CN solvent.

All the three complexes displayed intense bands within the range 334-440 nm and 576-660 nm. The trans complex showed an intense band ($\varepsilon \approx 10000$ $M^{-1}cm^{-1}$)

in the region 428-440 nm and 646-660 nm were assigned to the $t_2(Ru) \rightarrow \pi^*(L)$ (MLCT) transition. The cis complexes existed in two isomeric forms and both exhibited highly intense ($\varepsilon \approx$ 10000-30000 $M^{-1}cm^{-1}$) MLCT transitions at higher energies compared to the trans complex. An interesting trend in the MLCT band's feature between the trans and the cis complexes are as follows. The cis complexes displayed two different intense band characters. The most intense bands were in the range 334-364 nm and the less intense bands were in the range 576-584 nm. While, the spectrum of the trans complex showed two similar band characters. These intense bands were believed to be the spin-allowed singlet-singlet transition. Figure 13, 14 and 15 show the UV-Visible absorption spectra for all the three complexes in CH_3CN solvent.

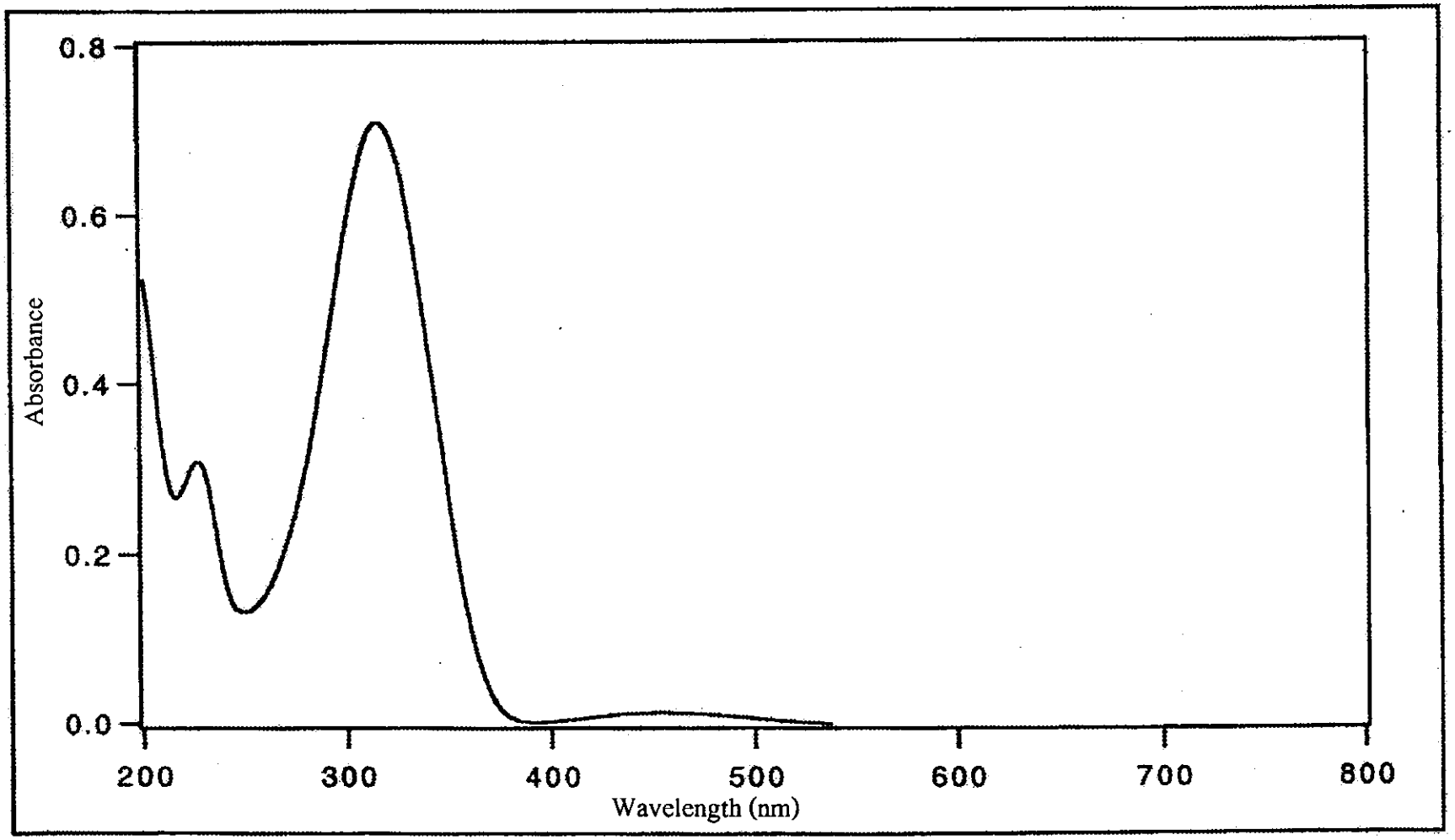

Figure 11. UV-Visible absorption spectrum of azine in CH_3CN.

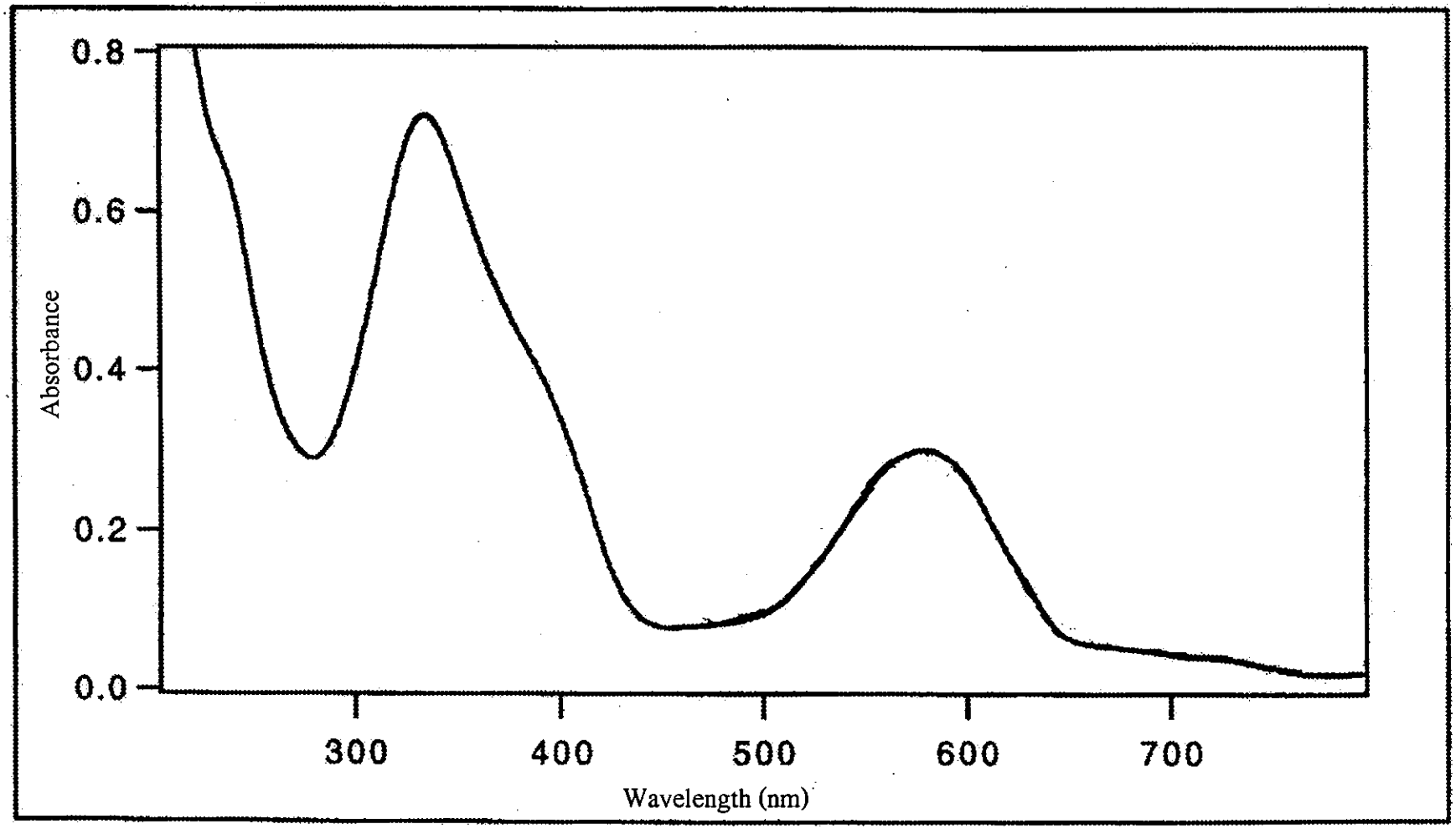

Figure 12. UV-Visible absorption spectrum of *ctc*-[Ru(azine)$_2$Cl$_2$] in CH_3CN.

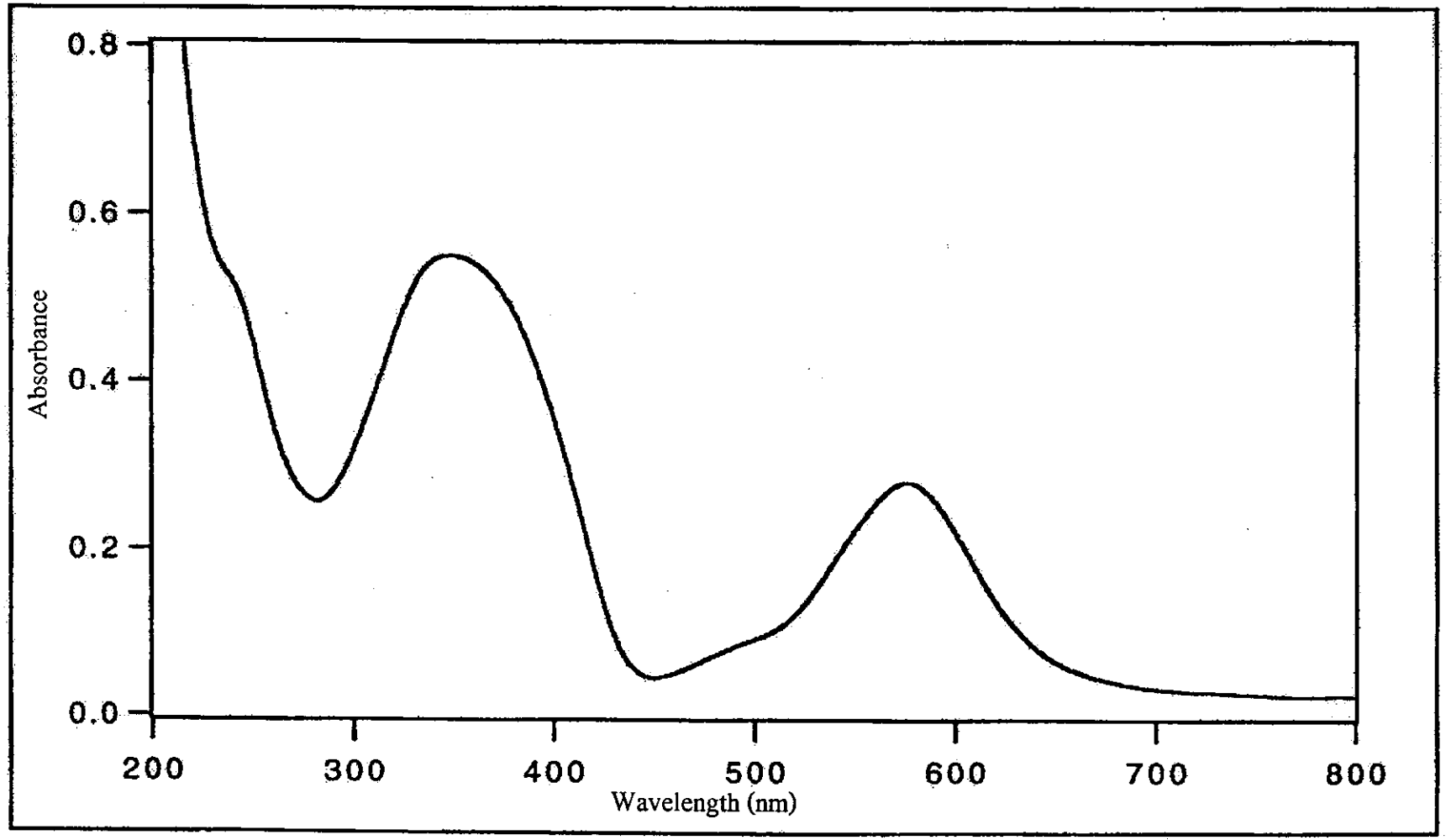

Figure 13. UV-Visible absorption spectrum of *ccc*-[Ru(azine)$_2$Cl$_2$] in CH_3CN.

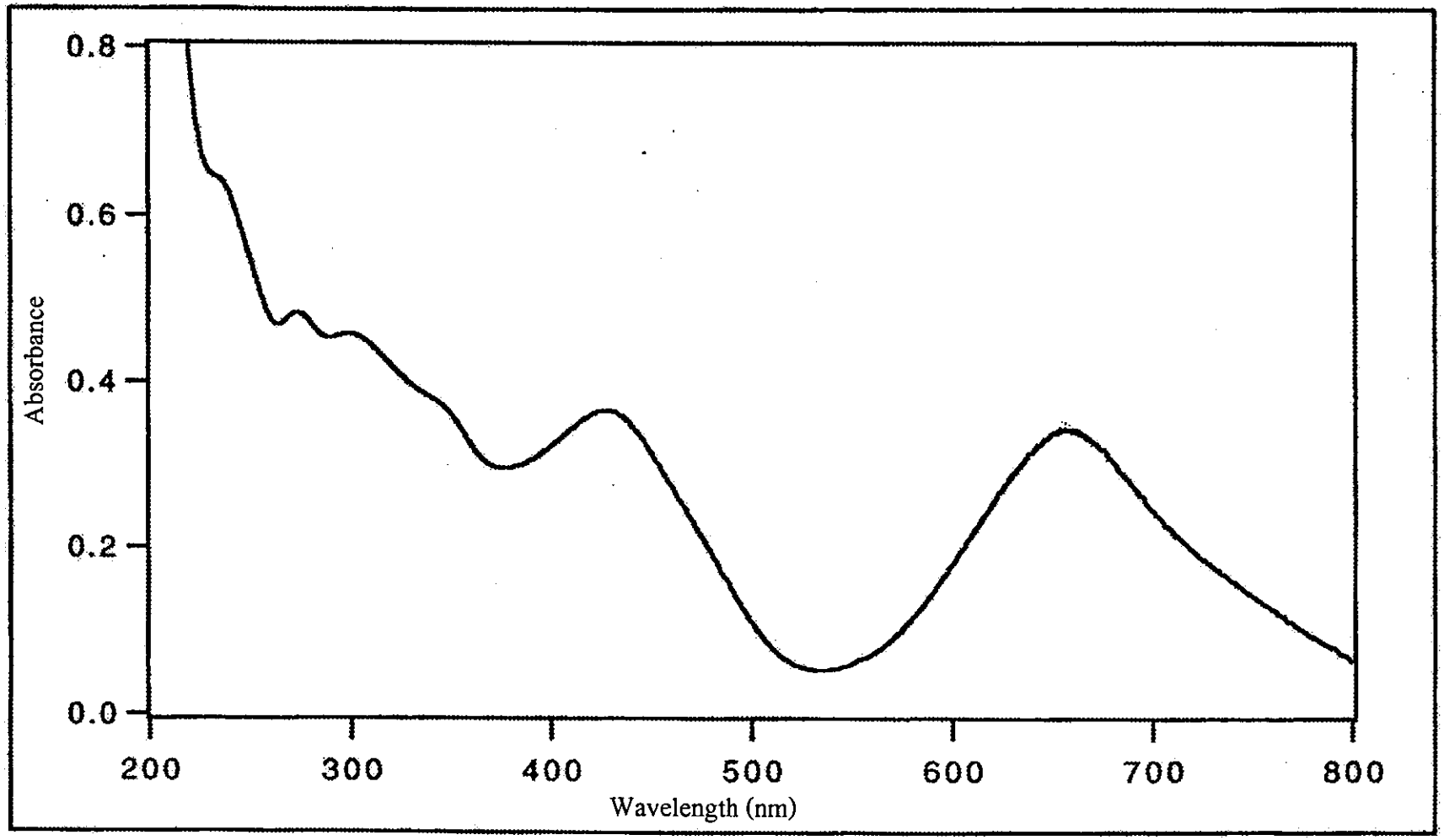

Figure 14. UV-Visible absorption spectrum of *tcc*-[Ru(azine)$_2$Cl$_2$] in CH_3CN.

3.2.5 Nuclear Magnetic Resonance spectroscopy (1D-2D)

Nuclear Magnetic Resonance (NMR) spectroscopy is a technique to determine molecular structure of compound. The structures of ligand and complexes were explained by using 1D and 2D NMR spectroscopic techniques (^{1}H NMR, ^{1}H-^{1}H COSY NMR, ^{13}C NMR, DEPT NMR and ^{1}H-^{13}C HMQC NMR). The NMR spectra of all compounds were recorded in $CDCl_3$ on UNITY SNOVA 500 MHz. The tetramethylsilane ($Si(CH_3)_4$) was used as an internal reference.

Nuclear Magnetic Resonance spectroscopy of the 2-(phenylazo)pyrazine ligand

Table 9. ^{1}H and ^{13}C NMR spectroscopic data of the azine ligand

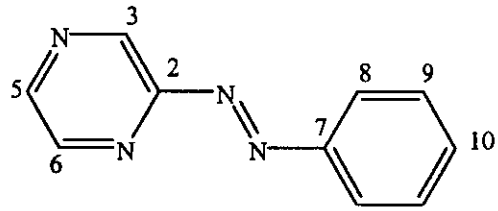

H-position	^{1}H NMR			^{13}C NMR
	δ(ppm)	J(ppm)	Number of H	(ppm)
3	9.1 (s)	-	1	138
5 6	8.7 (s)	-	2	143 145
8	8.1 (m)	-	2	123
9 10	7.5 (m)	-	3	129 132
Quaternary carbon				158 152

s = singlet, d = doublet, t = triplet

The ^{1}H NMR spectrum of the ligand was divided into two parts (Table 9). The downfield portion was due to the pyrazine protons (H3, H5, H6) and the upfield signals referred to azophenyl protons (H8, H9, H10). The proton H3 appeared as singlet peak at most downfield because it located next to the nitrogen atom. The signal of proton H5 and H6 occurred at the same position due to both protons located closed to each nitrogen atom. In the phenyl ring, the proton H8 were two equivalent protons. The signal occurred as doublet at 8.05 ppm. This resonance appeared at the lower field than the proton H9 and H10 because it located next to the azo nitrogen, the ^{1}H NMR spectrum of the azine ligand was shown in Figure 16. Moreover, also the peak assignment was done using simple correlation ^{1}H-^{1}H COSY NMR spectroscopy. The ^{1}H-^{1}H COSY NMR signals are presented in Figure 17.

The ^{13}C NMR (Figure 18) results corresponded to the those from DEPT NMR (Figure 19), which showed only methine carbon signals. The ^{13}C NMR spectrum of the azine ligand occurred 8 signals for 8 carbons. The quaternary carbon C2 of the pyrazine ring appeared at the most downfield. The signal at 152 ppm was due to the quaternary carbon C7 of the phenyl ring. The signals of carbon C3, C5 and C6 occurred at 138, 143 and 145 ppm, respectively. The carbon signals at 123 and 129 ppm were attributed to the two equivalent carbon C8 and C9. The signal carbon C10 appeared at 132 ppm. In addition, the signals of carbons in the phenyl ring occurred at the higher field than the pyrazine carbons. The ^{13}C NMR signals assignments were based on the ^{1}H-^{13}C HMQC NMR spectrum (Figure 20), which exhibited correlation between ^{1}H NMR spectrum and ^{13}C NMR spectrum.

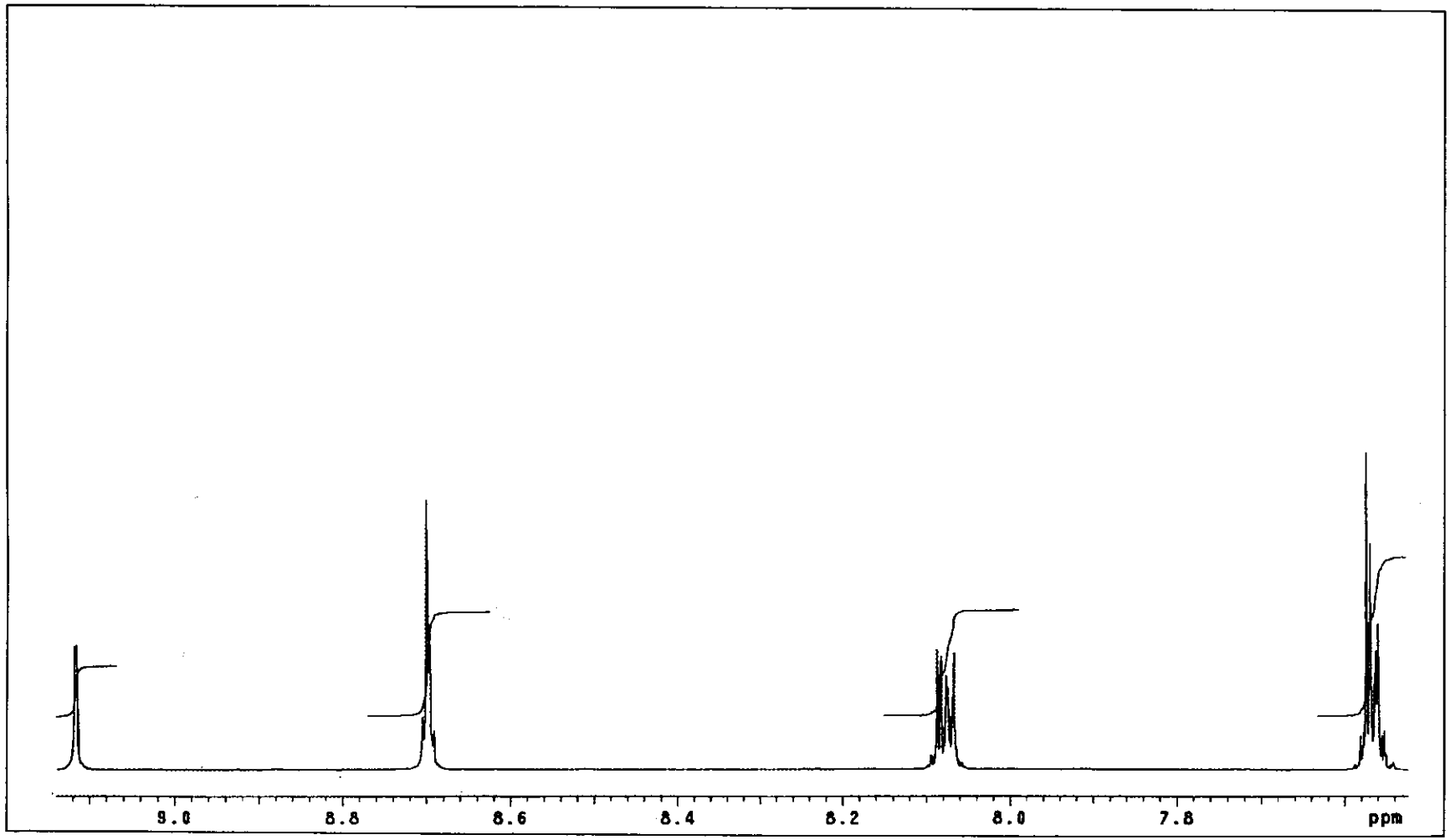

Figure 15. ^{1}H NMR spectrum of azine in $CDCl_3$.

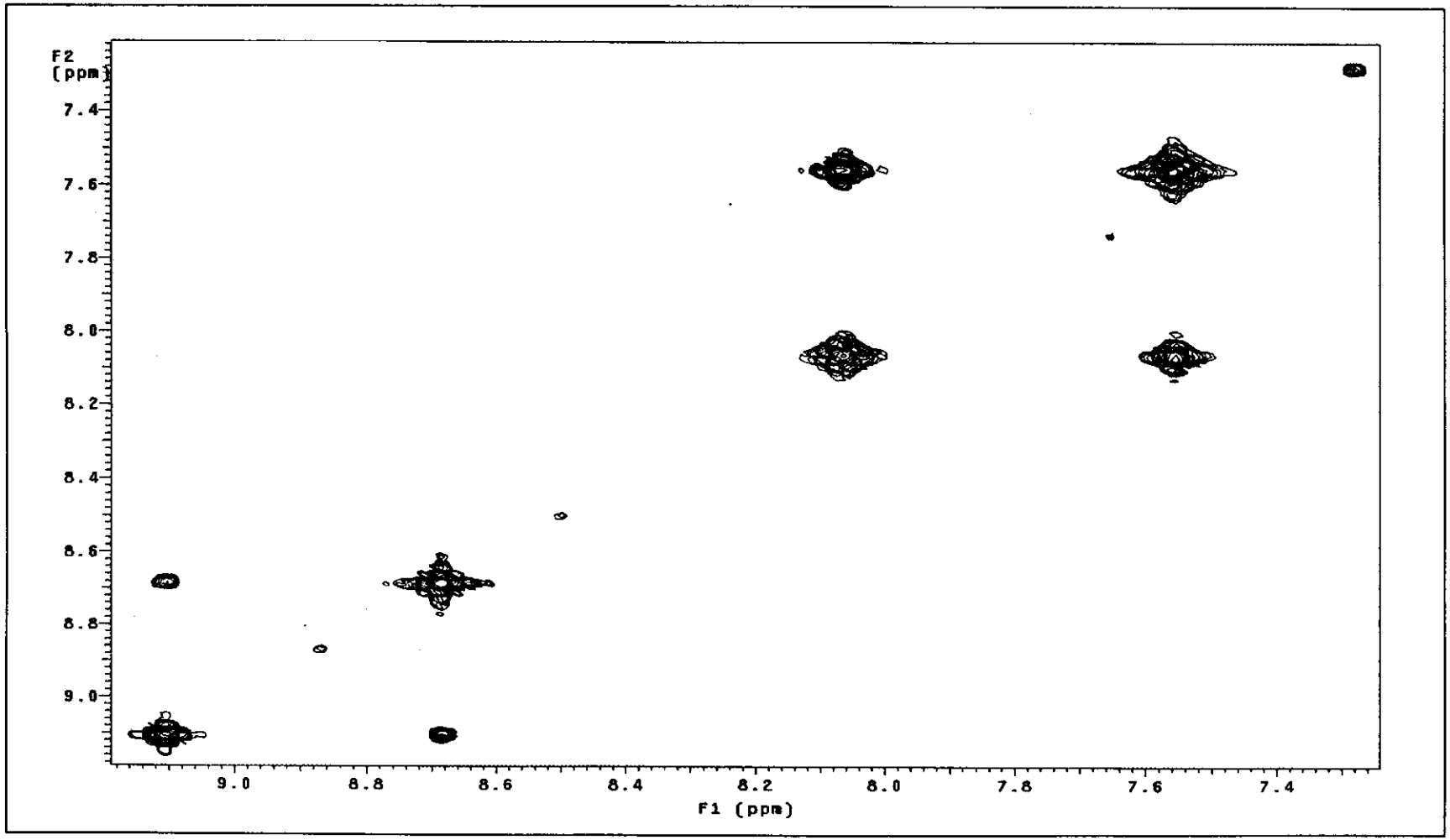

Figure 16. ^{1}H-^{1}H COSY NMR spectrum of azine in $CDCl_3$.

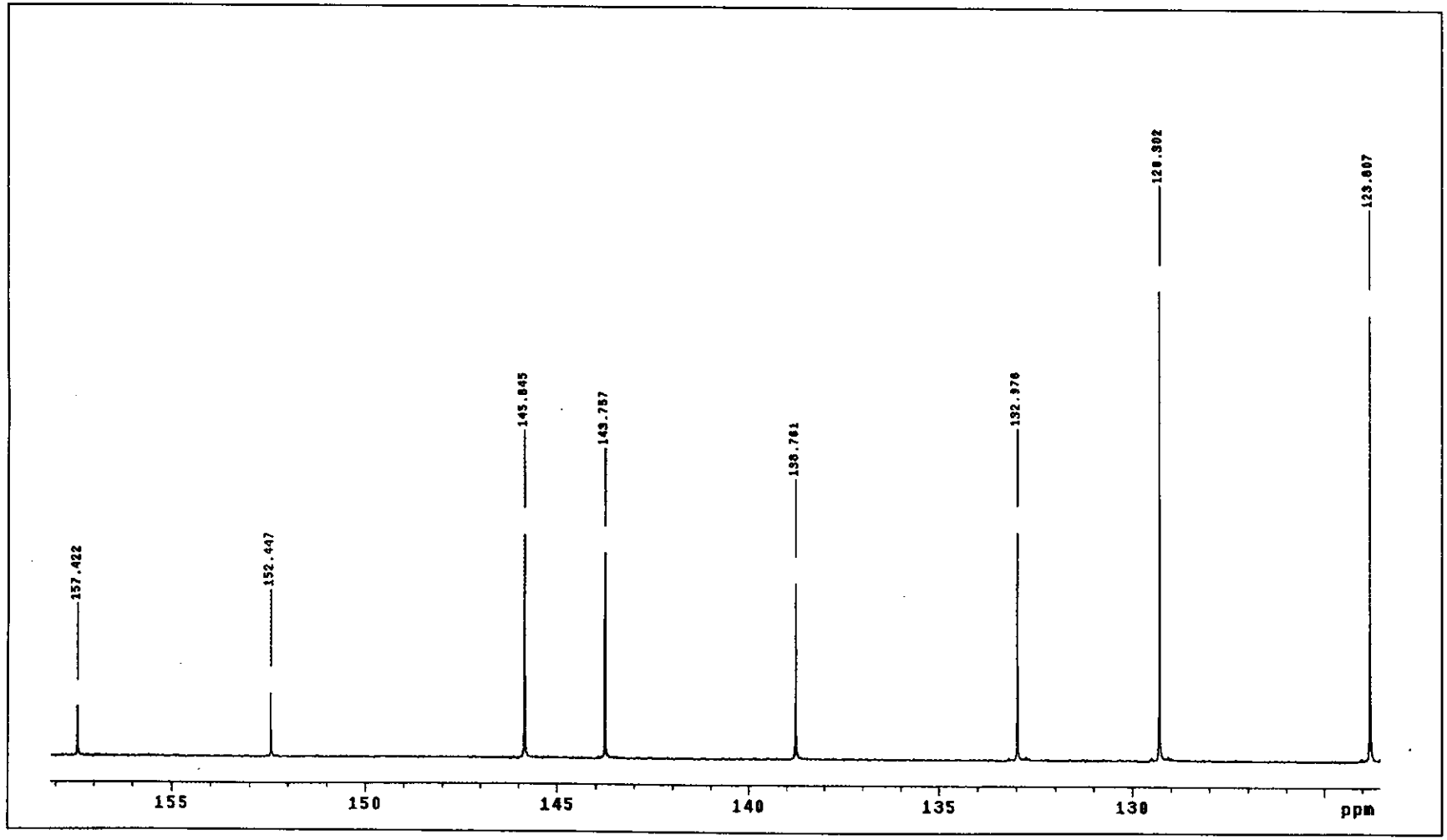

Figure 17. ^{13}C NMR spectrum of azine in $CDCl_3$.

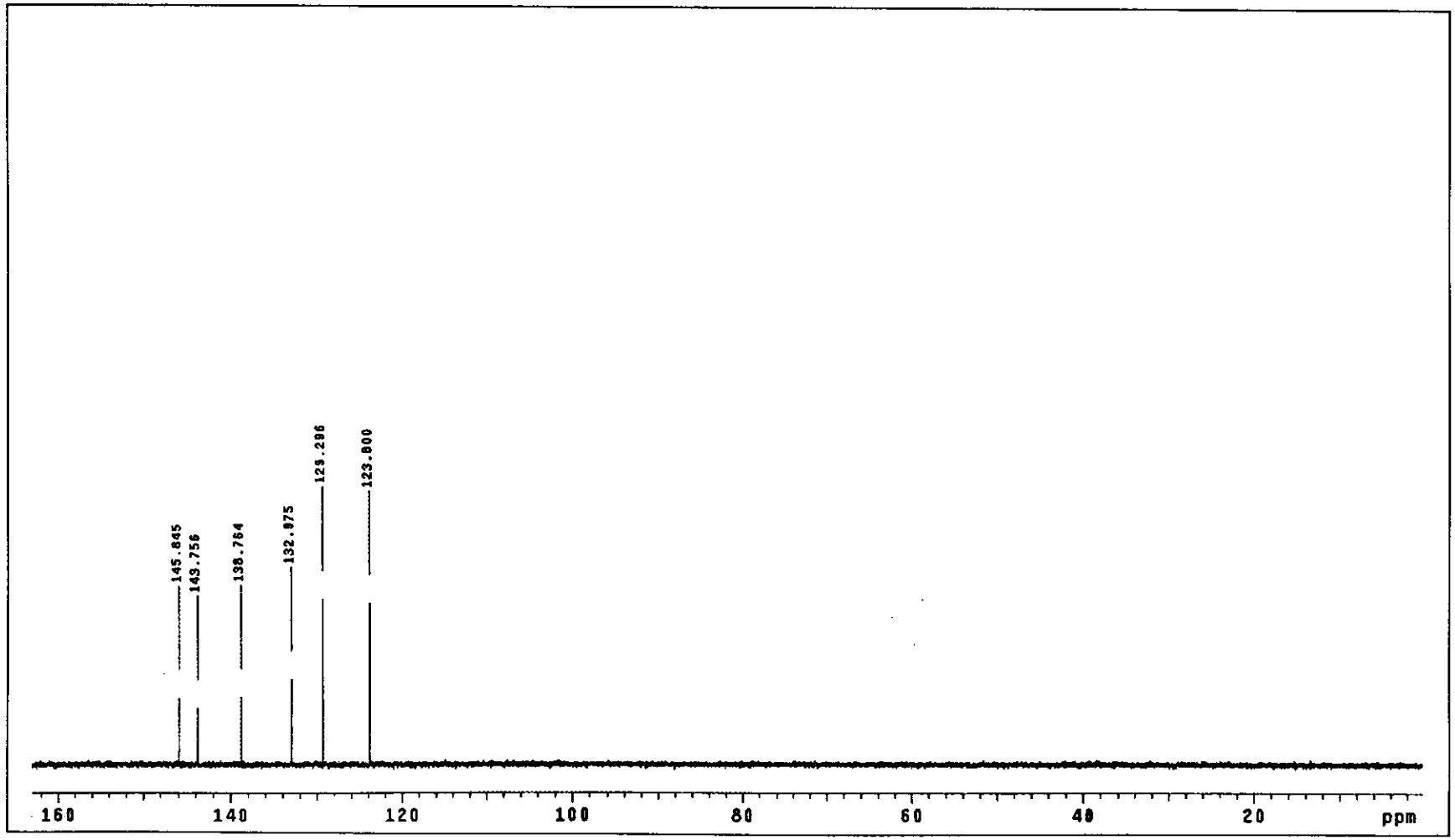

Figure 18. DEPT NMR spectrum of azine in $CDCl_3$.

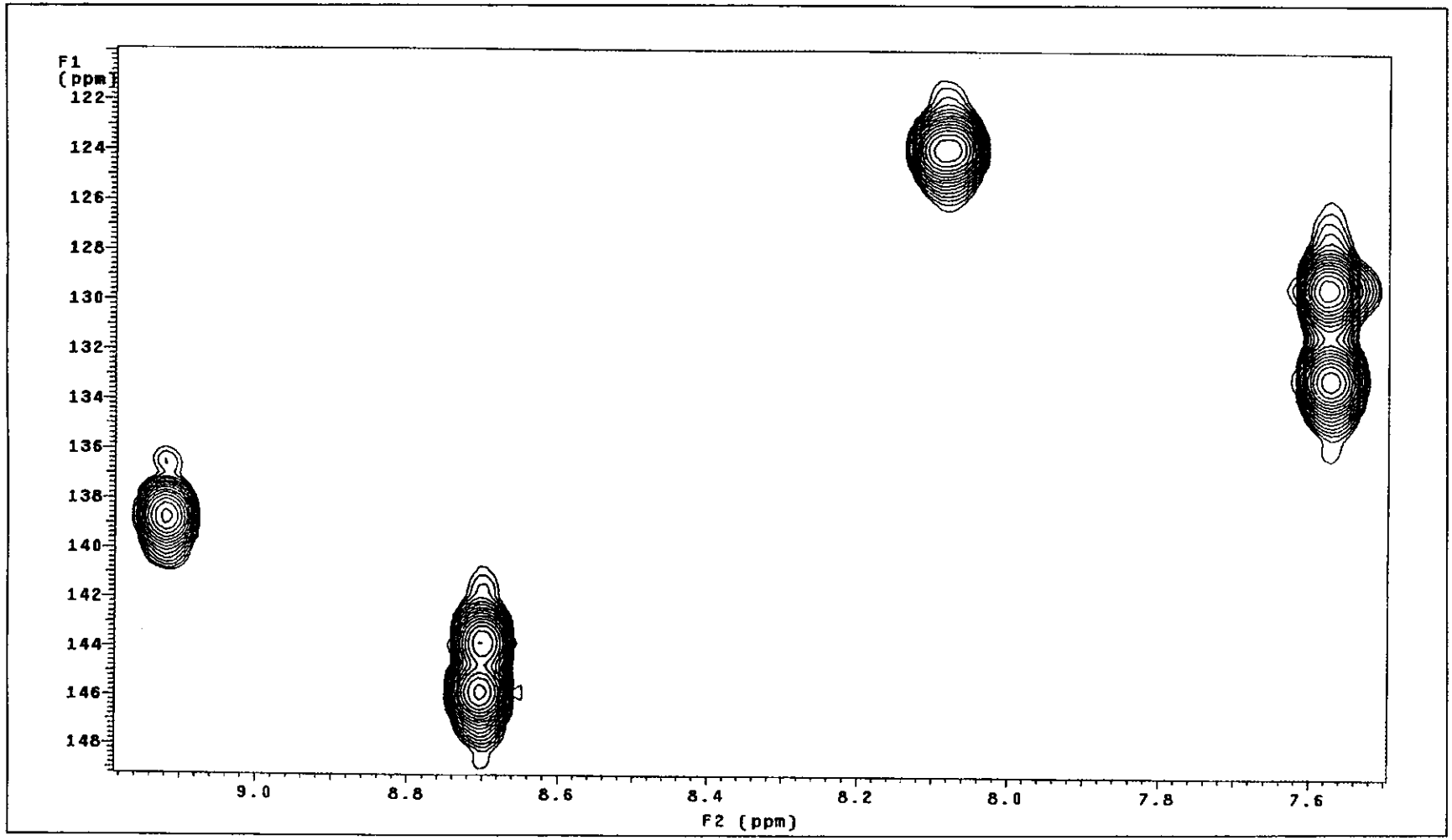

Figure 19. ^{1}H-^{13}C NMR spectrum of azine in $CDCl_3$.

Nuclear Magnetic Resonance spectroscopy of the *ctc*-[Ru(azine)$_2$Cl$_2$] complex

Table 10. ^{1}H and ^{13}C NMR spectroscopic data of the *ctc*-[Ru(azine)$_2$Cl$_2$] complex

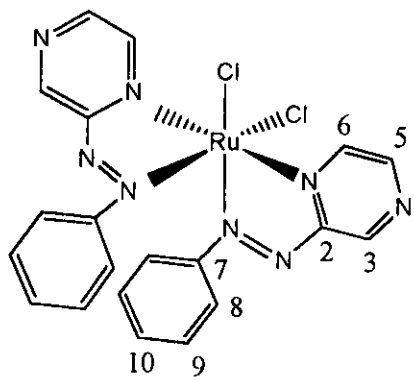

H-position	^{1}H NMR			^{13}C NMR
	δ(ppm)	J(ppm)	Number of H	(ppm)
3	9.7 (s)	-	1	147
6	9.4 (d)	3.5	1	145
5	8.7 (d)	3.0	1	144
10	7.3 (t)	7.5	1	131
9	7.1 (t)	8	2	128
8	6.7 (d)	7.5	2	121
Quaternary carbon				162 155

s = singlet, d = doublet, t = triplet

The ^{1}H NMR spectrum of *ctc*-[Ru(azine)$_2$Cl$_2$] complex appeared only one set of proton similar to the free ligand. This result indicated that the complex was a symmetric molecule (C_2-symmetry). Furthermore, the individual proton in molecule showed different chemical shifts. The signal of proton H3 in the pyrazine rings occurred at the lowest field due to the influence of coordinated nitrogen atoms. The

doublet peaks at 9.4 and 8.7 ppm were assigned to the signals of proton H6 and H5, respectively. The signals of proton H8, H9 and H10 on both phenyl rings appeared at the higher field than others. The doublet peak of proton H8 was observed at the most upfield. It was splitted by proton H9 (J = 7.5 Hz). The triplet peaks at 7.3 and 7.1 ppm were due to H10 and H9, respectively.

The ^{13}C NMR (Figure 23) result corresponded to the DEPT NMR (Figure 24) as same as these results of free ligand, but each signal slightly shifted to lower field or higher field than free ligand. The downfield signals at 162 and 155 ppm were assigned to two quaternary carbons C2 and C7, respectively. The methine carbons on the pyrazine rings occurred at the lower field than the phenyl rings. It was due to the effect of the nitrogen atoms. Moreover, the ^{13}C NMR signals assignment were based on the ^{1}H-^{13}C HMQC spectrum (Figure 25).

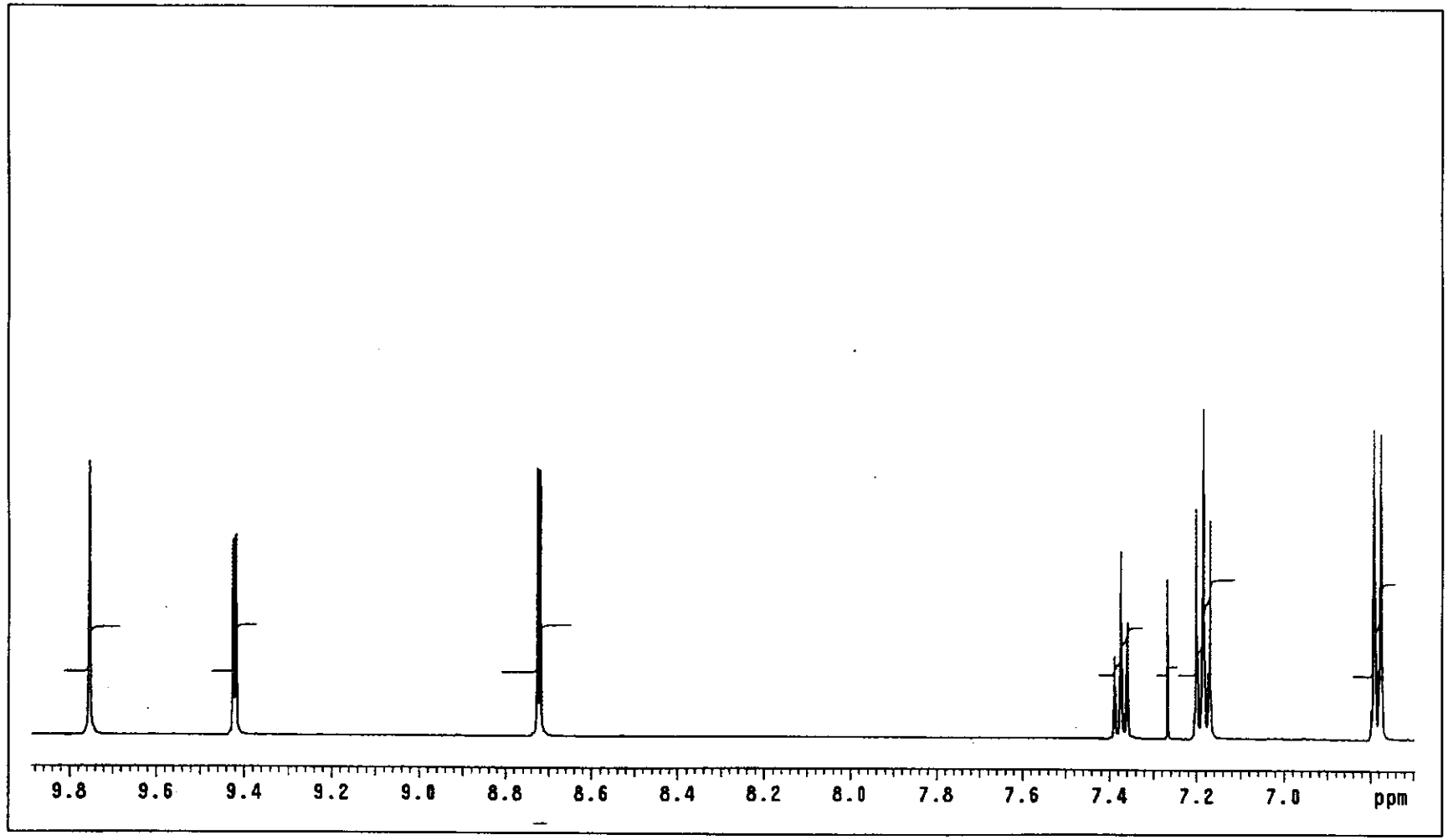

Figure 20. ^{1}H NMR spectrum of *ctc* -$[Ru(azine)_2Cl_2]$ in $CDCl_3$.

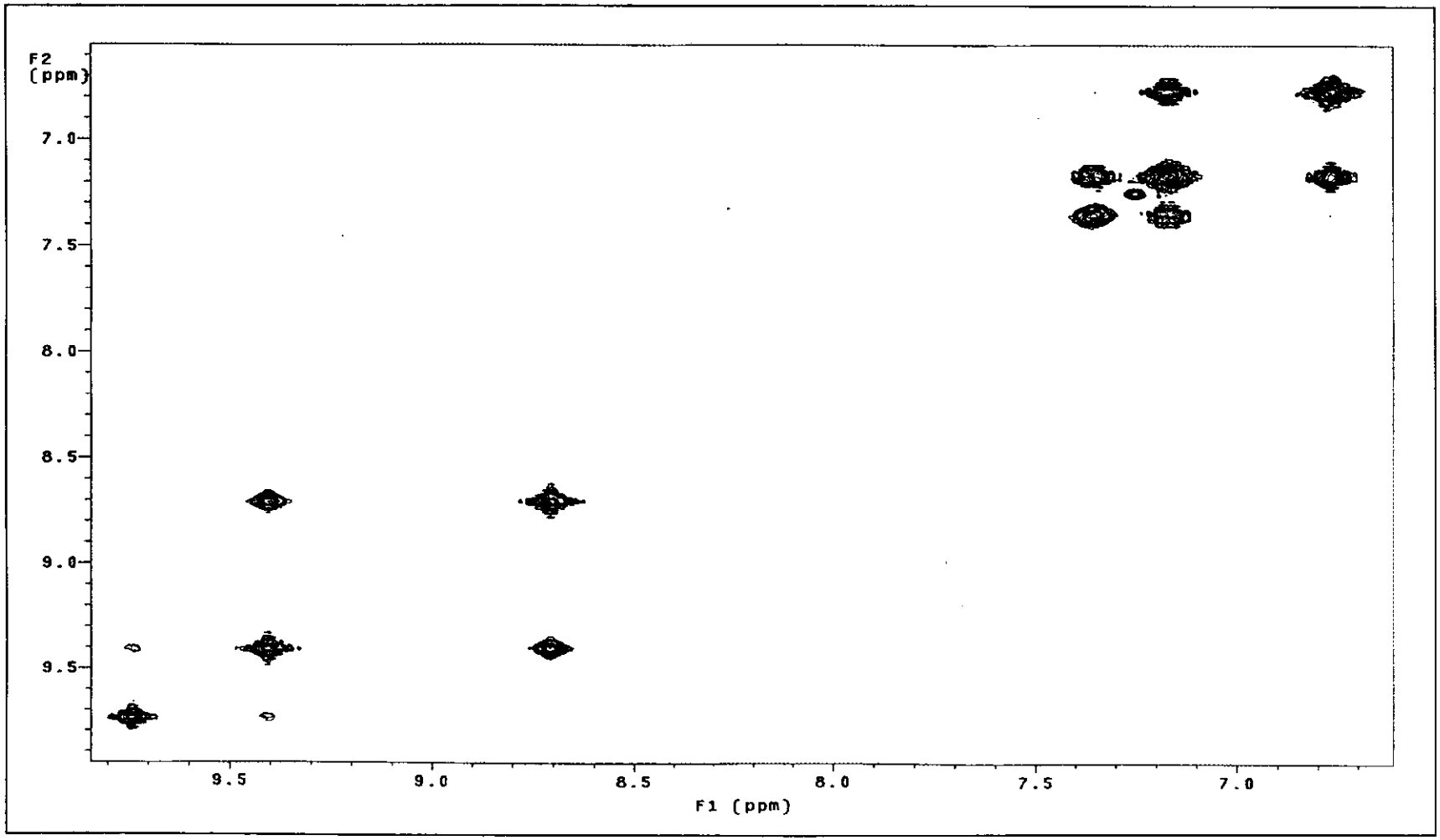

Figure 21. ^{1}H-^{1}H COSY NMR spectrum of *ctc* - $[Ru(azine)_2Cl_2]$ in $CDCl_3$.

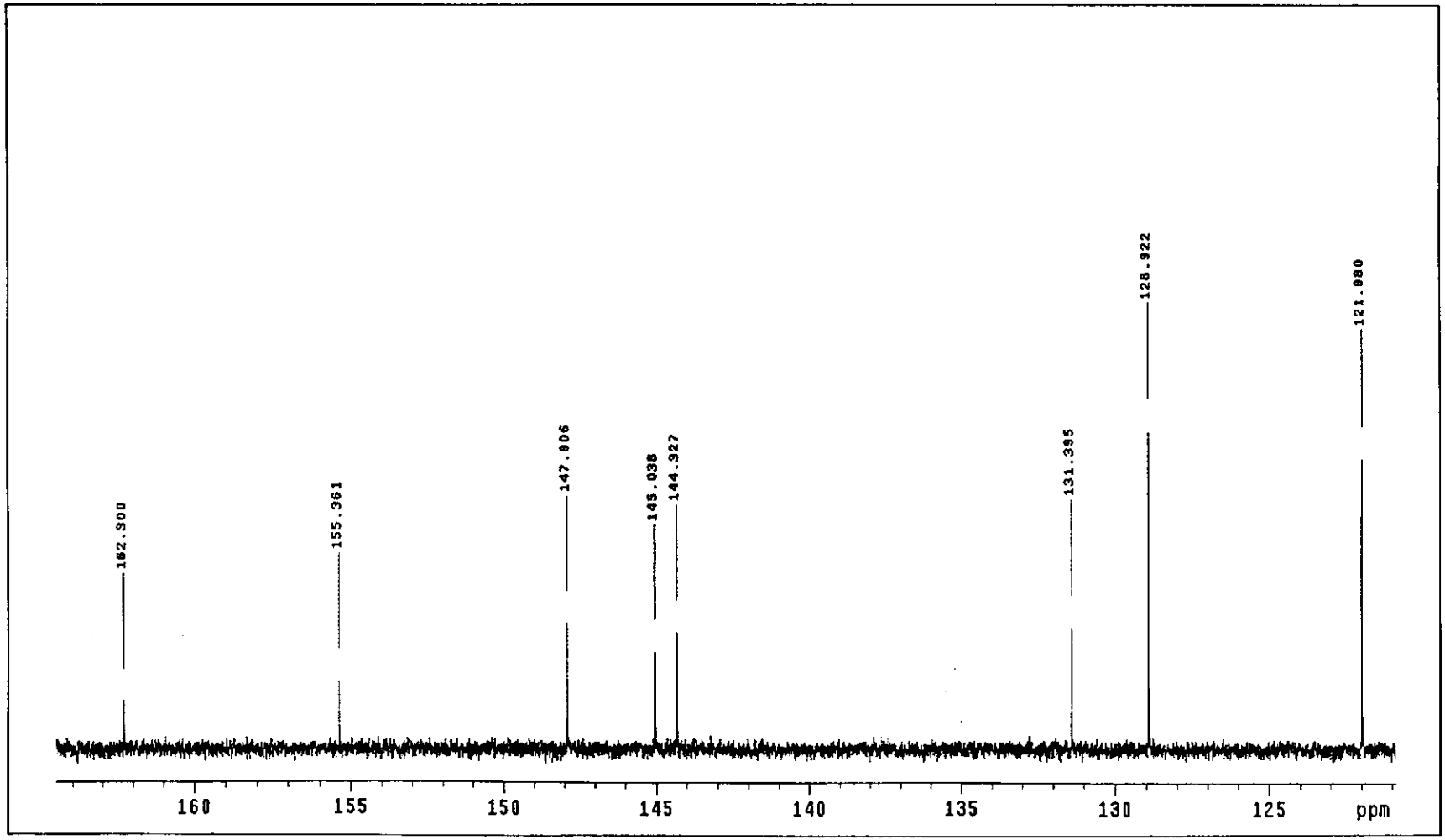

Figure 22. ^{13}C NMR spectrum of *ctc* - $[Ru(azine)_2Cl_2]$ in $CDCl_3$.

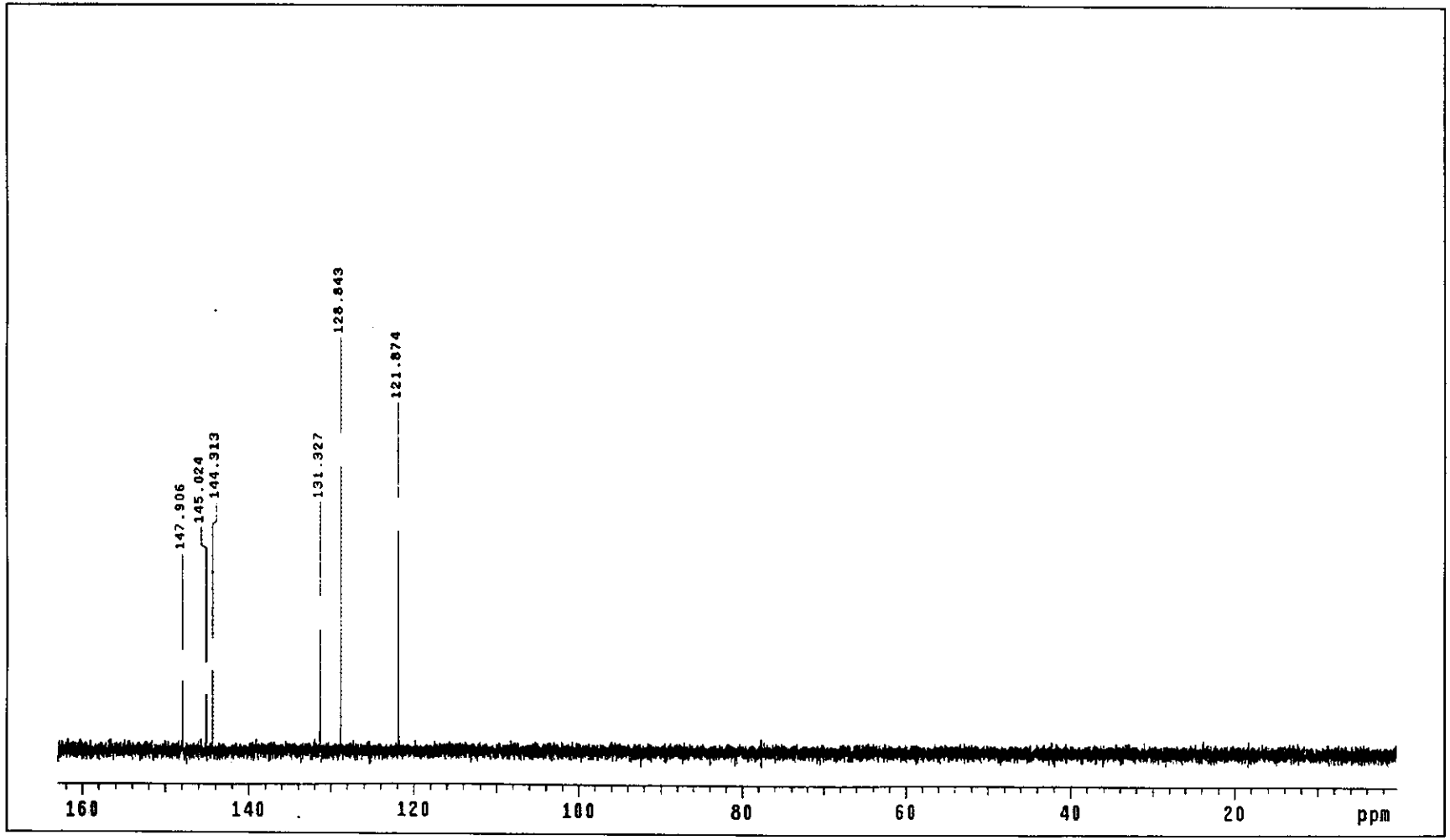

Figure 23. DEPT NMR spectrum of *ctc* - $[Ru(azine)_2Cl_2]$ in $CDCl_3$.

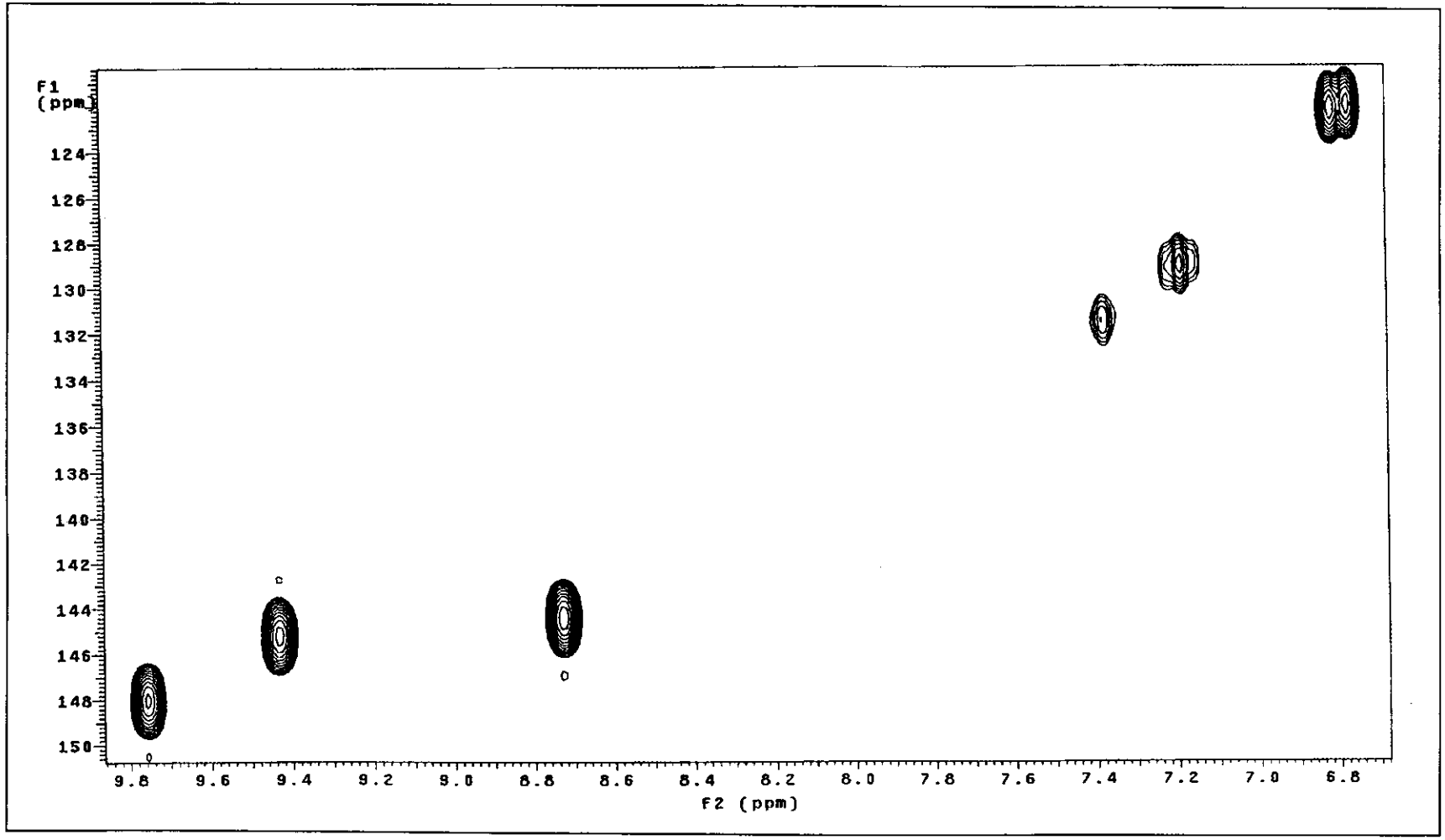

Figure 24. ^{1}H- ^{13}C HMQC NMR spectrum of *ctc* - $[Ru(azine)_2Cl_2]$ in $CDCl_3$.

Nuclear Magnetic Resonance spectroscopy of the *ccc*-[Ru(azine)$_2$Cl$_2$] complex

Table 11. ^{1}H and ^{13}C NMR spectroscopic data of the *ccc*-[Ru(azine)$_2$Cl$_2$] complex

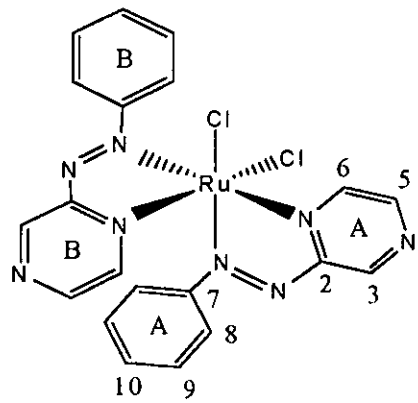

H-position	^{1}H NMR			^{13}C NMR
	δ(ppm)	J(ppm)	Number of H	(ppm)
3(A)	9.8 (s)	-	1	147
3(B)	9.7 (s)	-	1	146
6(A)	9.8 (d)	3.0	1	144
6(B)	8.5 (d)	3.3	1	143
5(A)	9.1 (d)	3.0	1	144
5(B)	7.3 (d)	3.3	1	142
8(A)	7.9 (d)	8.5	2	126
8(B)	6.8 (d)	8.5	2	121
9(A)	7.4 (t)	8.1, 7.2	2	129
9(B)	7.2 (t)	8.4, 7.5	2	127

Table 11. (continued)

H-position	^{1}H NMR			^{13}C NMR
	δ(ppm)	J(ppm)	Number of H	(ppm)
10(A)	7.6 (t)	7.2, 7.5	1	132
10(B)	7.4 (t)	7.5, 7.5	1	131
Quaternary carbon				162 162 157 155

s = singlet, d = doublet, t = triplet

In the spectrum of *ccc*-[Ru(azine)$_2$Cl$_2$] showed two sets of protons (Figure 26). It was due to C_1-symmetry of the complex. The pyrazine protons H3(A) and H3 (B) were observed at different chemical shifts. The proton H3 in pyrazine ring A appeared at the lower field than pyrazine ring B because it was trans to N=N withdrawing group. In addition, the proton in phenyl ring A occurred at the lower field than phenyl ring B because it was trans to electron withdrawing group, chloride. The proton H8(B) was observed at the highest field. Figure 27 showed ^{1}H-^{1}H COSY NMR spectrum of this complex.

The ^{13}C NMR spectrum (Figure 28) showed 12 methine carbons and 4 quaternary carbons. The DEPT spectral data (Figure 29) presented only signal of methine carbons and supported ^{13}C NMR result.

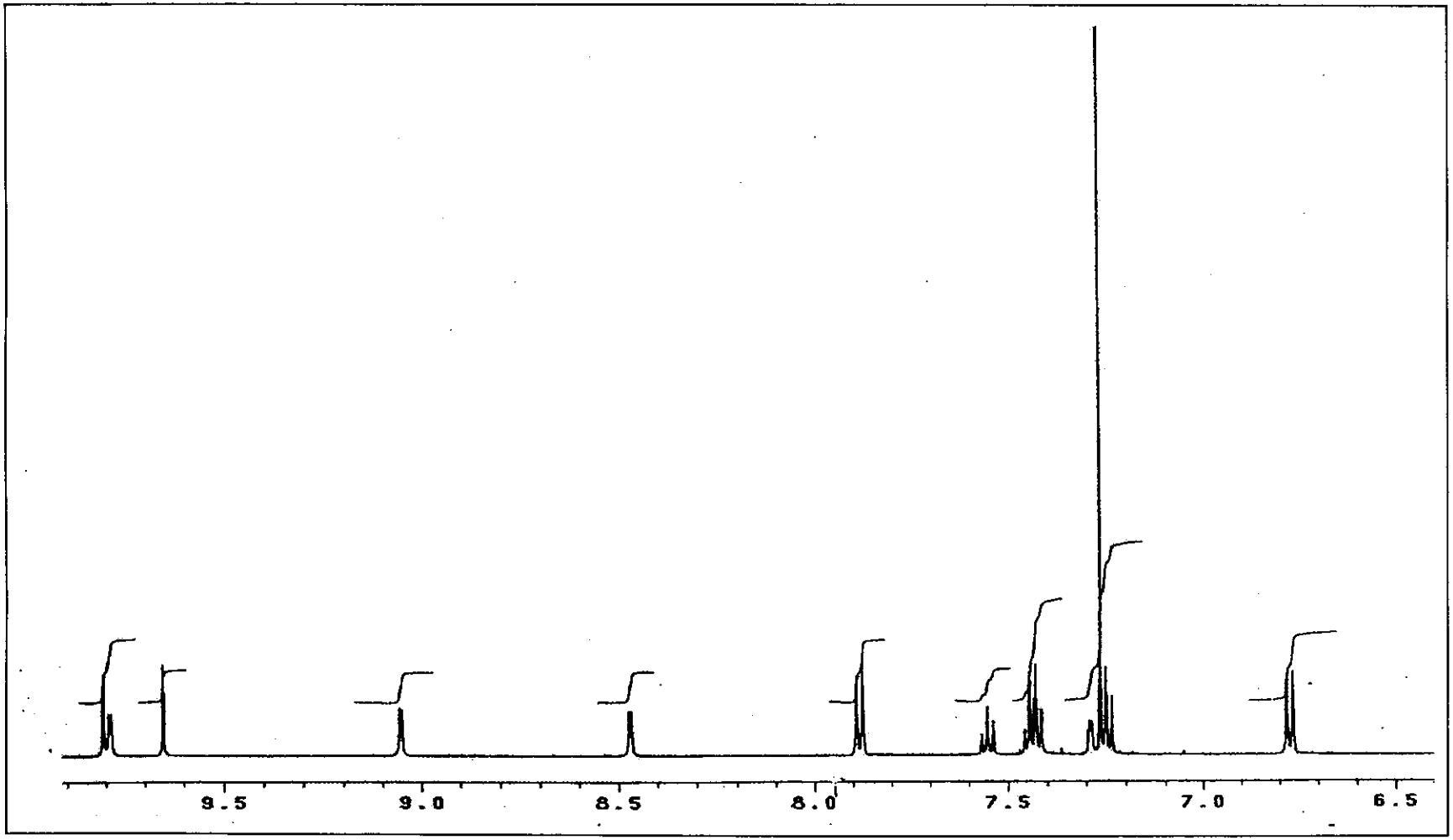

Figure 25. ^{1}H NMR spectrum of *ccc*-[Ru(azine)$_2$Cl$_2$] in $CDCl_3$.

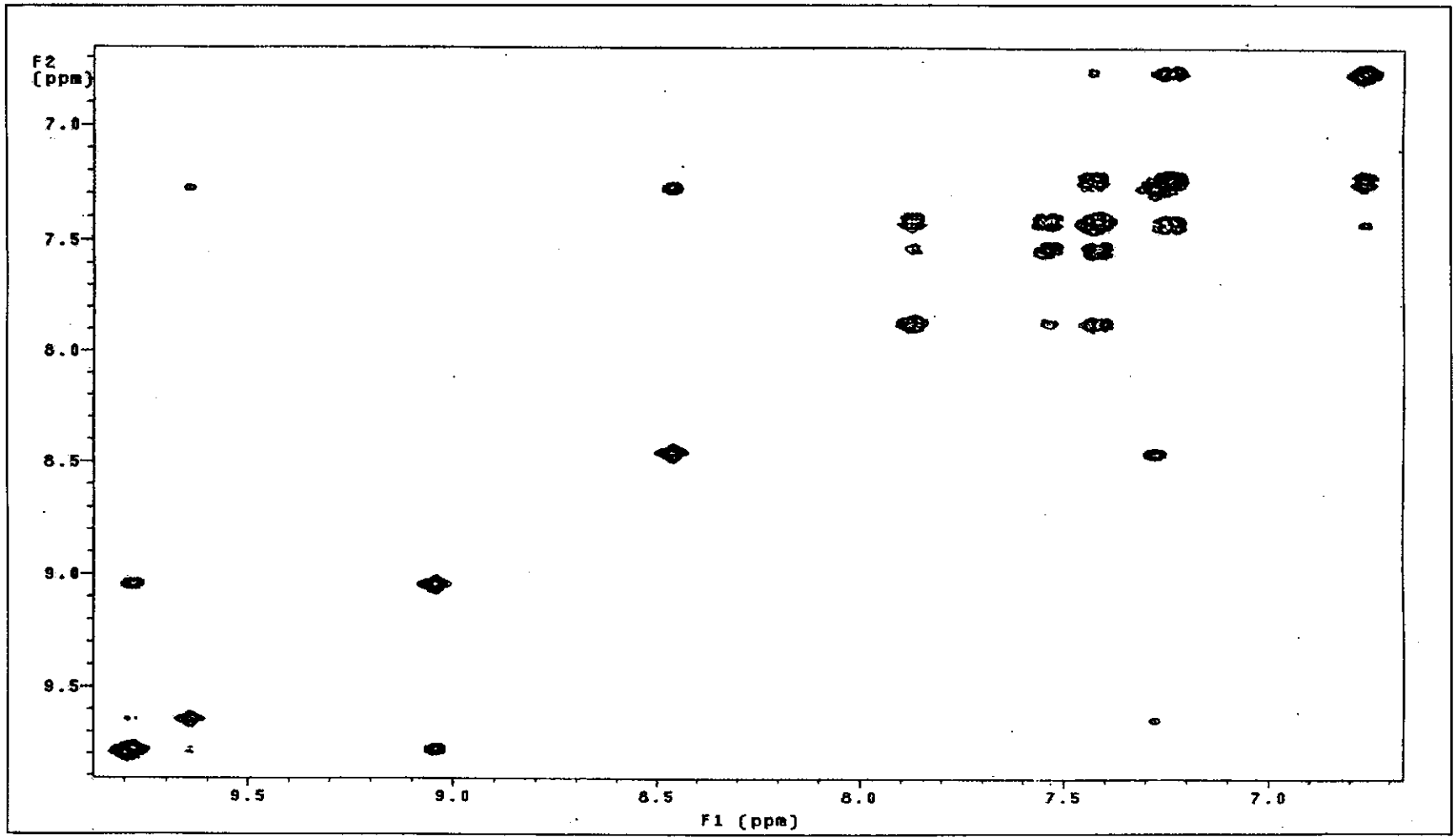

Figure 26. ^{1}H-^{1}H COSY NMR spectrum of *ccc*-[Ru(azine)$_2$Cl$_2$] in $CDCl_3$.

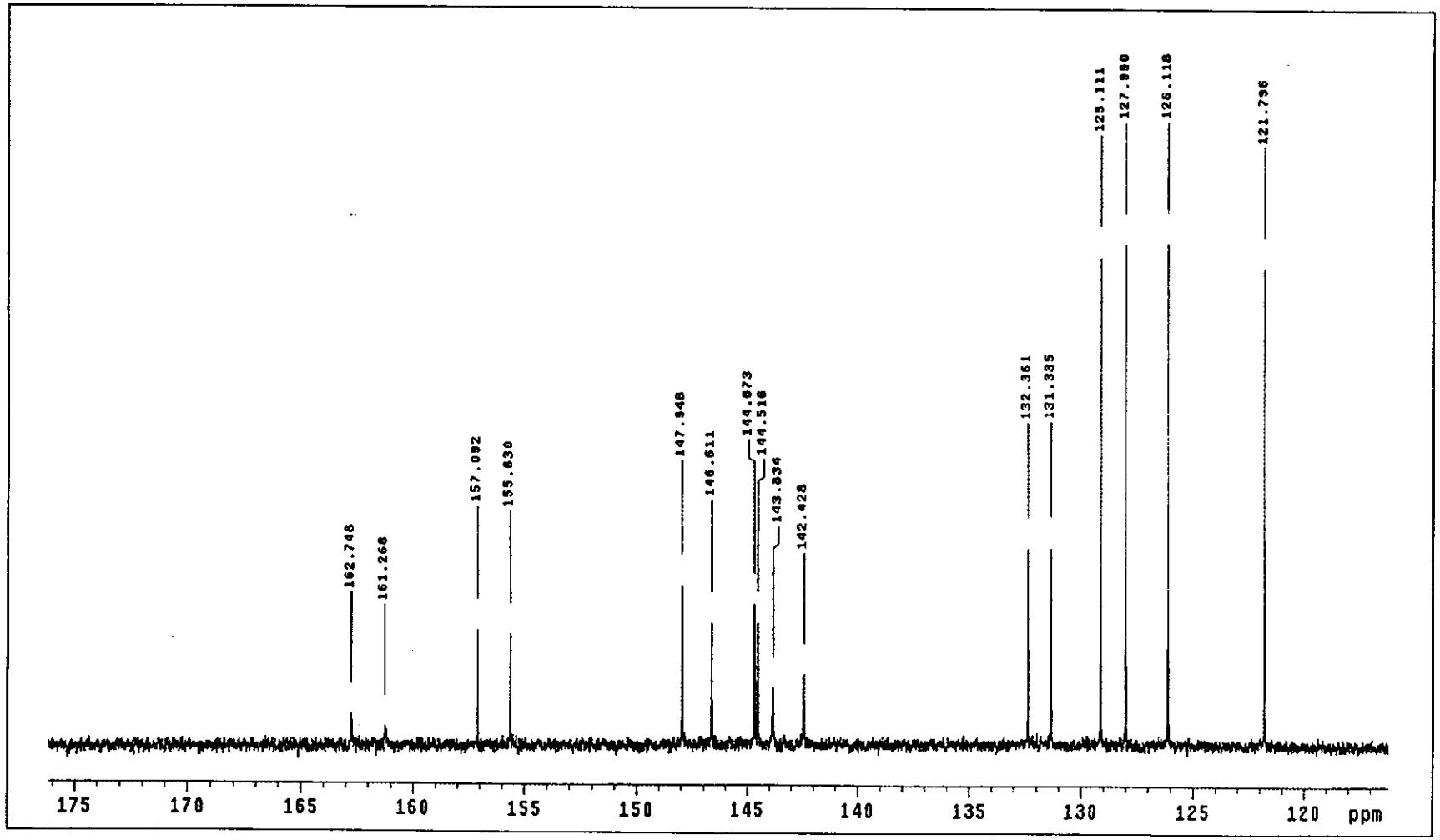

Figure 27. ^{13}C NMR spectrum of *ccc* -[Ru(azine)$_2$Cl$_2$] in $CDCl_3$.

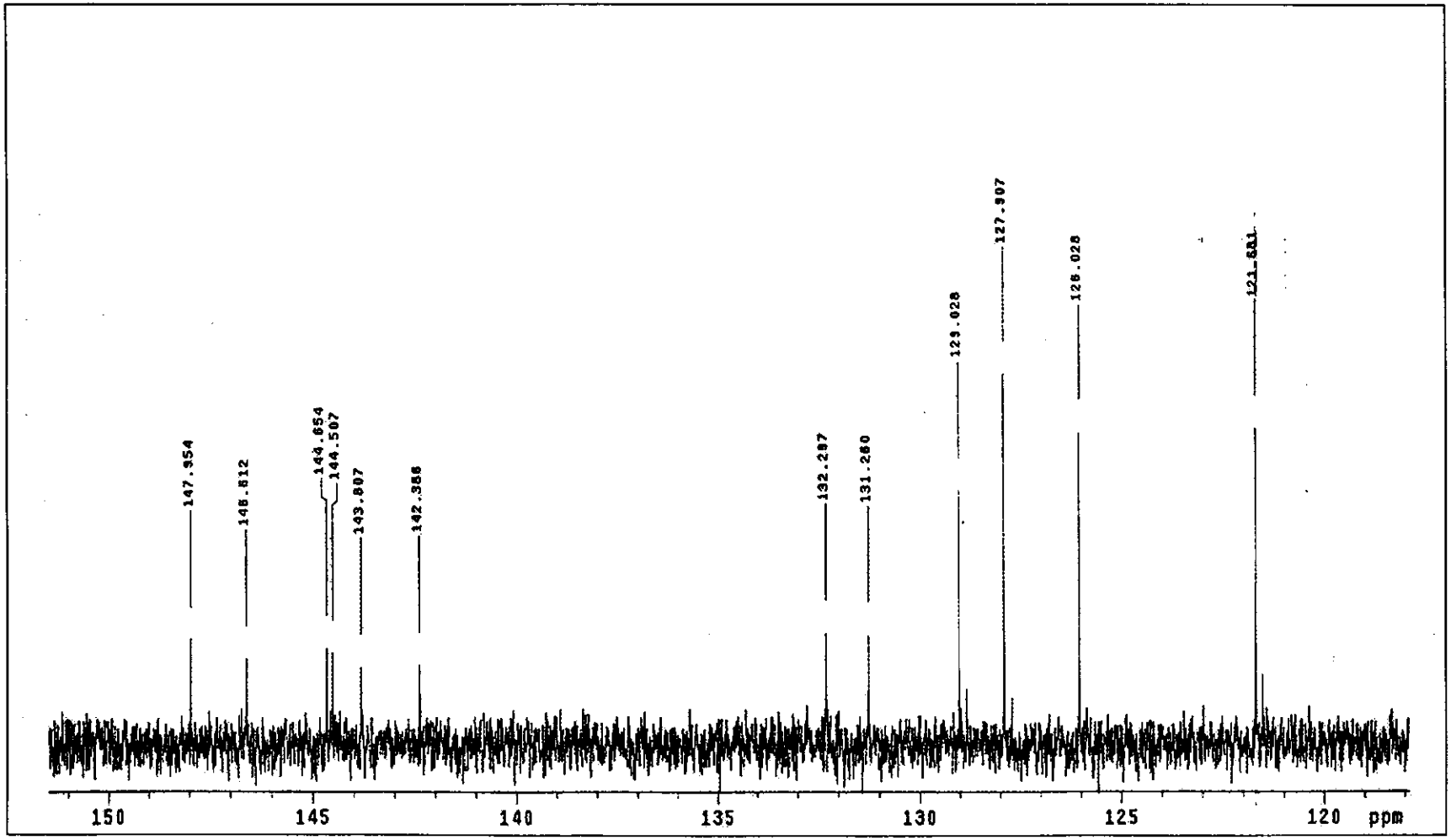

Figure 28. DEPT NMR spectrum of *ccc*-[Ru(azine)$_2$Cl$_2$] in CDCl$_3$.

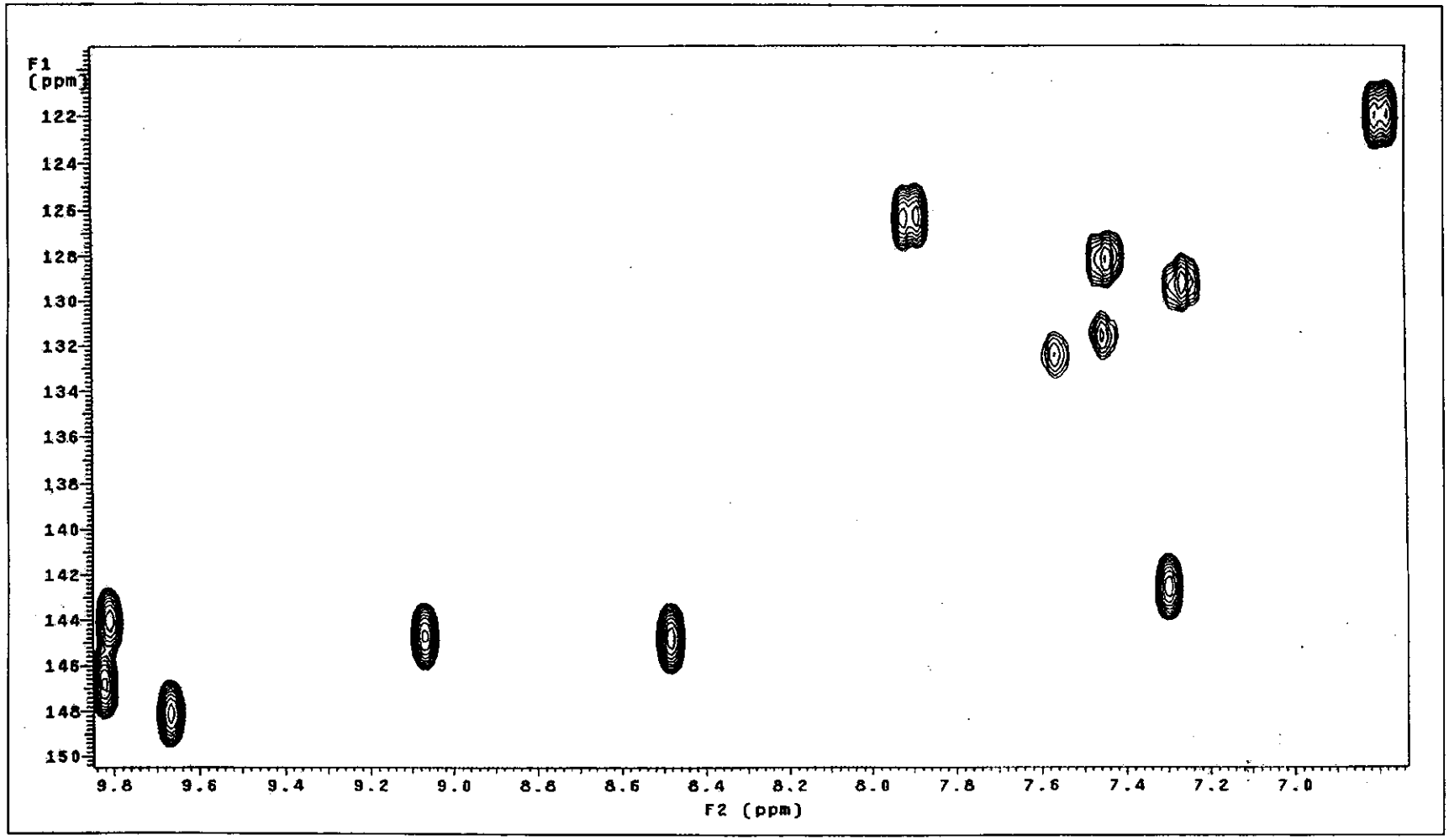

Figure 29. ^{1}H- ^{13}C HMQC NMR spectrum of *ccc*-[Ru(azine)$_2$Cl$_2$] in $CDCl_3$.

Nuclear Magnetic Resonance spectroscopy of the *tcc*-[Ru(azine)$_2$Cl$_2$] complex

Table 12. ^{1}H and ^{13}C NMR spectroscopic data of the *tcc*-[Ru(azine)$_2$Cl$_2$] complex

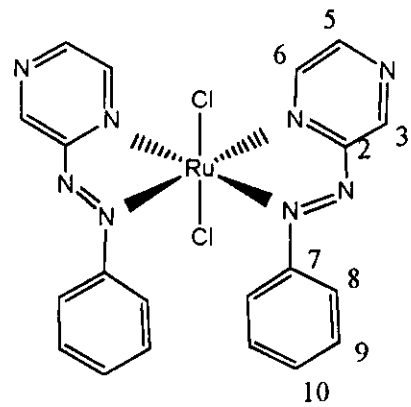

H-position	^{1}H NMR			^{13}C NMR
	δ(ppm)	J(ppm)	Number of H	(ppm)
3	9.8 (s)	-	1	146
6	9.0 (d)	3.0	1	143
5	8.9 (d)	3.5	1	143
8	7.5 (d)	8.5	2	123
10	7.2 (t)	7.5	1	130
9	7.0 (t)	8.0	2	128
Quaternary carbon				160 158

s = singlet, d = doublet, t = triplet

The ^{1}H NMR spectrum of the *tcc*-[Ru(azine)$_2$Cl$_2$] complex showed only one set of protons (Figure 31) because this molecule also has C_2-symmetry. The pyrazine protons occurred at the lower field than the phenyl protons. The singlet peak at the most down field was assigned to the proton H3. The doublet peaks of protons H5 and H6 occurred at 8.9 and 9.0 ppm. The triplet peak of proton H9 appeared at the

highest field. It was splitted by proton H10 and H9 (J = 8 Hz). A doublet and a triplet were observed at 8.5 and 7.5 ppm, respectively. The former was assigned to the proton H8 and the latter was assigned to the proton H10. In addition, this complex was also studied by using simple correlation 1H-1H COSY NMR spectroscopy (Figure 32).

The ^{13}C NMR spectrum is shown in Figure 33. The spectrum of the *tcc*-[Ru(azine)$_2$Cl$_2$] complex occurred at the position as same as the *ctc*-[Ru(azine)$_2$Cl$_2$] complex. The quaternary carbon C2 and C7 were observed at 160 and 158 ppm, respectively. The carbon C3 signal occurred at 146 ppm, which was lower field than carbon C5 and C6. The phenyl carbon C8, C9 and C10 appeared at 123, 128 and 130 ppm, respectively.

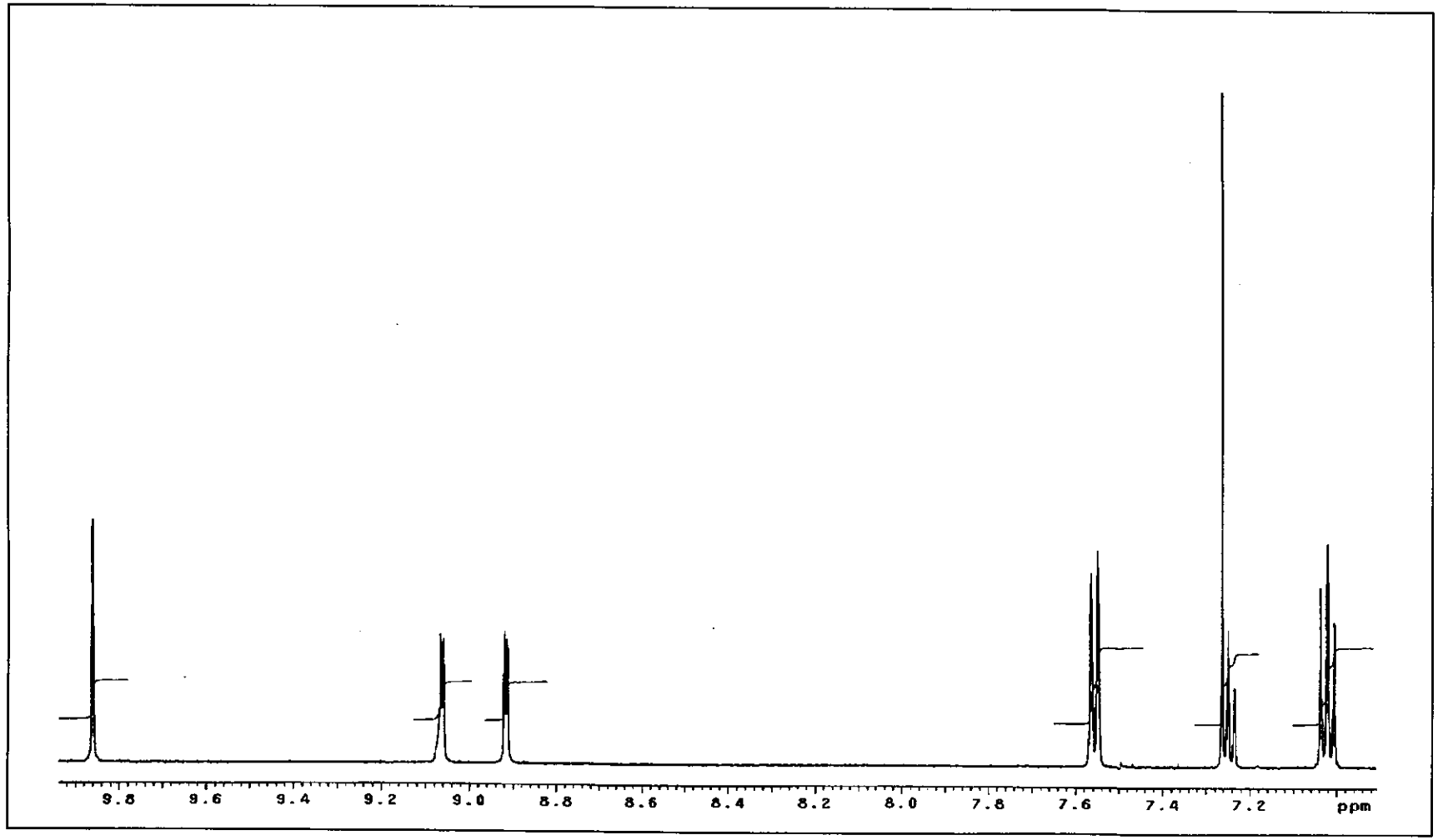

Figure 30. ^{1}H NMR spectrum of *tcc*-[Ru(azine)$_2$Cl$_2$] in $CDCl_3$.

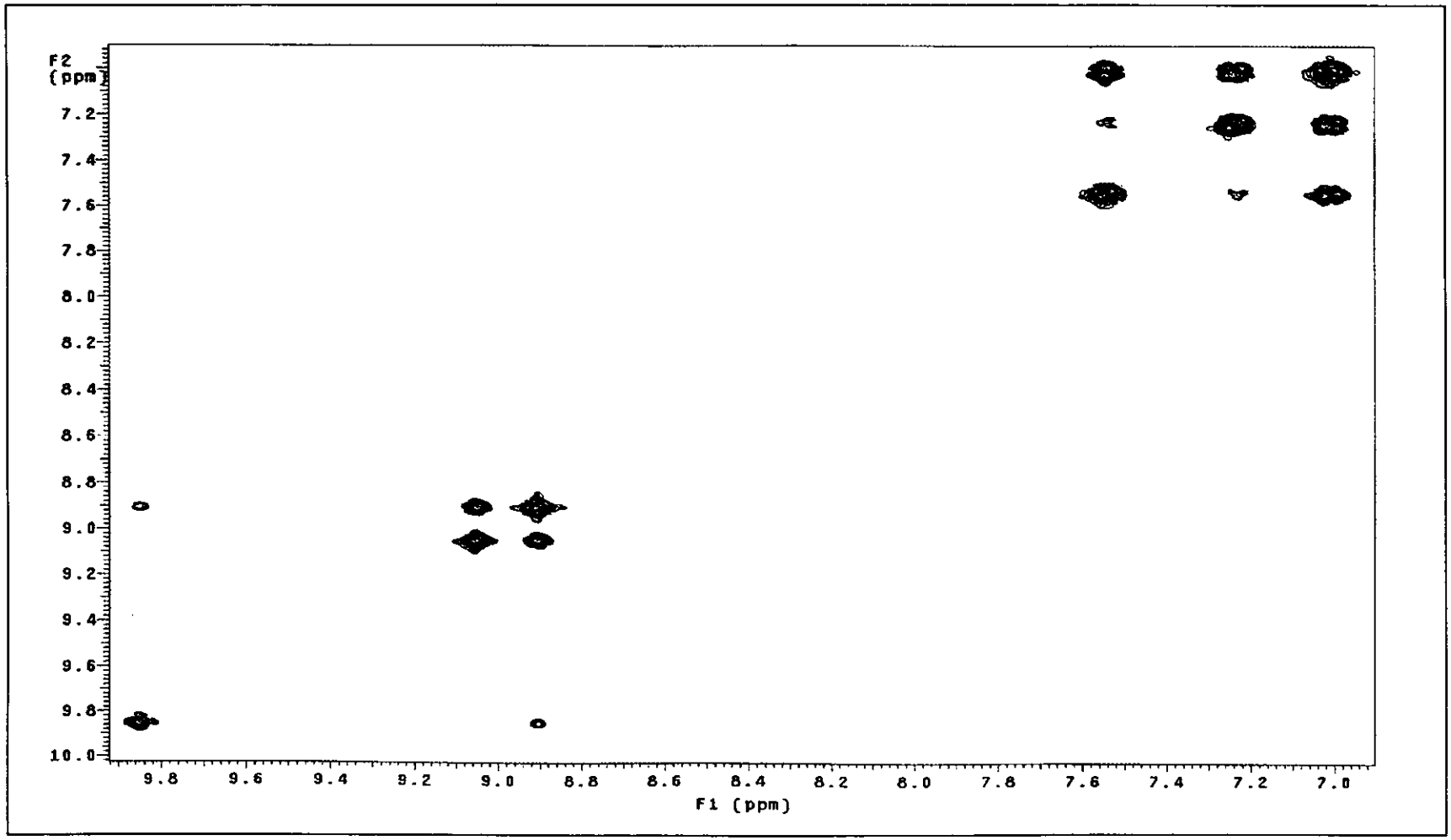

Figure 31. ^{1}H-^{1}H COSY NMR spectrum of *tcc*-[Ru(azine)$_2$Cl$_2$] in $CDCl_3$.

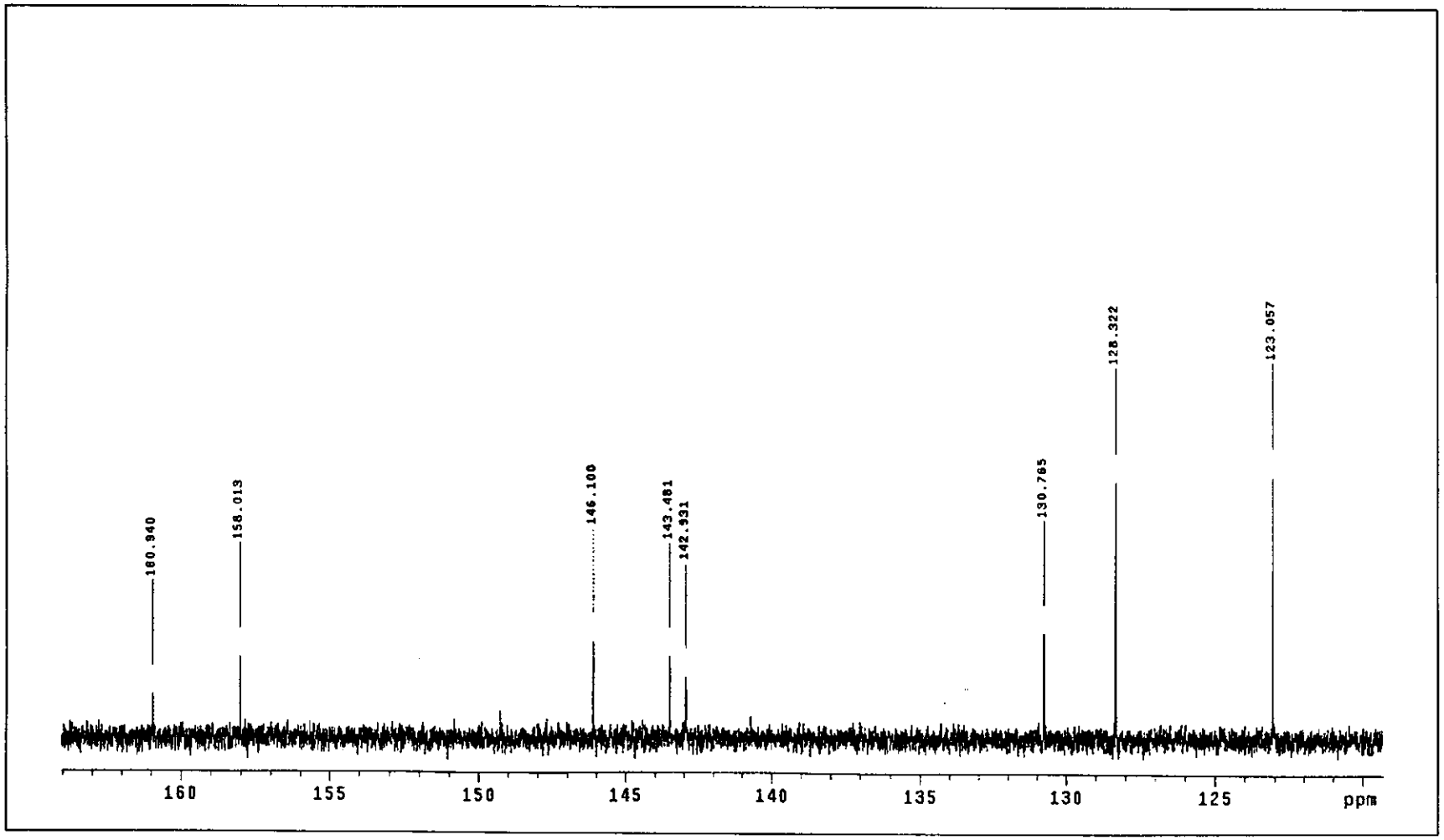

Figure 32. ^{13}C NMR spectrum of *tcc*-[Ru(azine)$_2$Cl$_2$] in $CDCl_3$.

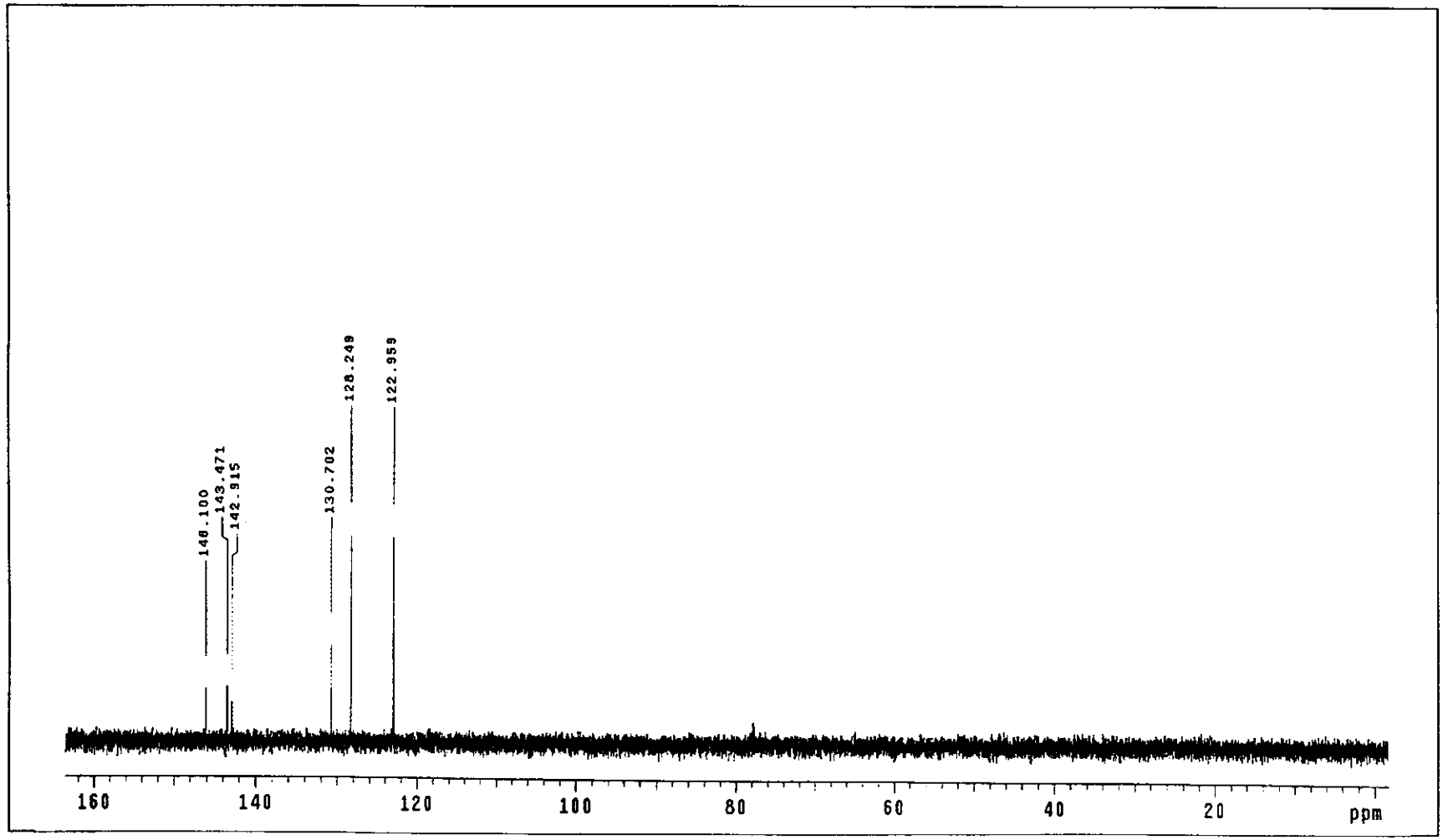

Figure 33. DEPT NMR spectrum of *tcc*-[Ru(azine)$_2$Cl$_2$] in $CDCl_3$.

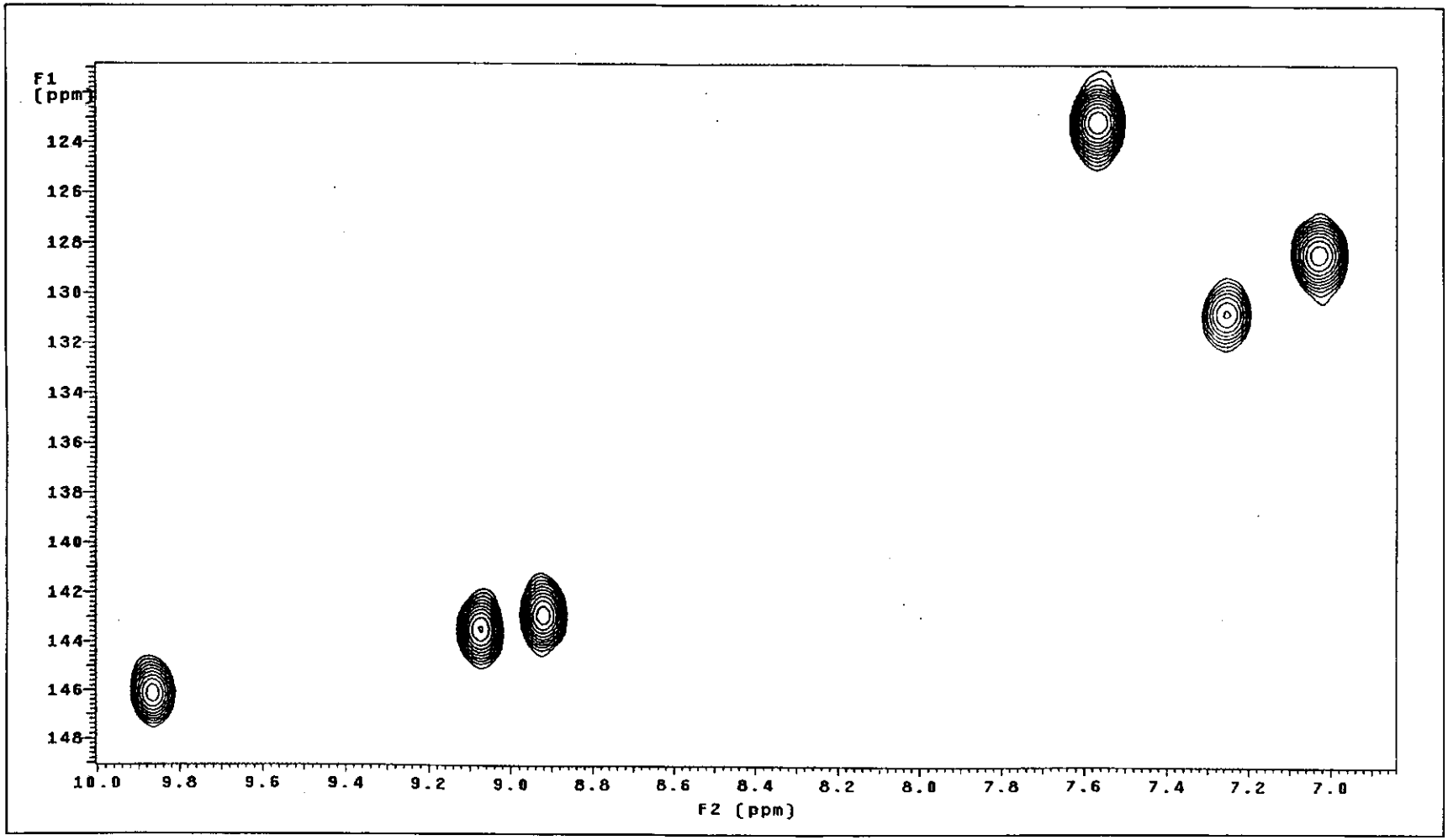

Figure 34. ^{1}H- ^{13}C HMQC NMR spectrum of *tcc*-[Ru(azine)$_2$Cl$_2$] in $CDCl_3$.

3.2.6 Cyclic Voltammetry

The electrochemical behaviour of the complexes in CH_3CN was examined by cyclic voltammetry. The cyclic voltammogram displayed metal oxidations on the positive side and ligand reductions on the negative side. The potentials were compared with the potential of ferrocene couple. The results are given in Table 13 and the representative voltammograms are shown in Figure 36 to 39.

In this experiment, the different scan rates were used to check the couple or the redox reaction. The couple having almost equal anodic and cathodic current was referred to reversible couple. On the other hand, the unequal currents were referred to the unequally transfer of electron in reduction and oxidation. This led to irreversible couple. When different scan rates were applied, these currents gave equal anodic and cathodic currents at higher scan rate, which led to quasi-reversible couple.

Table 13. Cyclic voltammetric[a] data for the azine ligand and the three complexes in 0.1 M TBAH acetonitrile at scan rate 50 mV/s

Compound	$E_{1/2}$ (V) (ΔE_p(mV))		
	Oxidation	Reduction	
azine	-	-1.28 (270)	
ctc-[Ru(azine)$_2$Cl$_2$]	0.95 (180)	-0.66 (90)	-0.99[b]
ccc-[Ru(azine)$_2$Cl$_2$]	0.93 (125)	-0.72 (80)	-1.04[b]
tcc-[Ru(azine)$_2$Cl$_2$]	0.77 (70)	-0.59 (145)	-0.98[b]

[a] $E_{1/2} = (E_{pa} + E_{pc})/2$, where E_{pa} and E_{pc} are anodic and cathodic peak potentials, respectively; $\Delta E_p = E_{pa} - E_{pc}$

[b] cathodic peak potential, V

In the oxidation range +0.5 to +1.5 V at scan rate 50 mV/s, one electron oxidation response was observed corresponding to the Ru(II) $\longrightarrow$ Ru(III) couple at the platinum disc electrode surface. The oxidation process is shown in equation (1).

$$Ru(azine)_2Cl_2 \longrightarrow Ru(azine)_2Cl_2^+ + e^- \qquad (1)$$

The data (Table 13) reveal that the blue complexes (ctc and ccc) exhibited higher potentials by 0.18-0.16 V than the green (tcc) complex. Then, the Ru(II)$\longrightarrow$(III) oxidation in the cis isomers became more positive and were observed at higher potential than the trans isomer. The ctc isomer showed a slightly higher Ru(III)/Ru(II) couple (0.02 V) than that of the ccc isomer. These were also supported by electronic spectral data.

In the potential range -0.5 to –1.5 V, reductive responses were observed. The reduction potentials were compared with the results from the free ligand. The free ligand displayed one quasi-reversible two electron reduction response with peak to peak separation at 270 mV, corresponded to the couple in equation (2).

$$azine \overset{2e^-}{\rightleftharpoons} azine^{2-} \qquad (2)$$

The potential of this couple was –1.28 V, which was more positive than the azopyridine (-1.61 V) analogues by 0.32 V but occurred close to the azopyrimidine ligand (-1.14 V) by 0.14 [Santra, *et al.*, 1999]. All the three complexes displayed one quasi-reversible, one electron reduction, and one irreversible peak of one electron. Moreover, the reduction potential showed a positive shifted from the free ligand value. The first reduction couple of the tcc complex (-0.59 V) occurred at higher potential than that in the ctc (-0.66 V) and the ccc (-0.72 V.) complexes. These results showed

that the tcc isomer accepted electron better than the cis isomers. In addition, it could be concluded that the azine ligand in tcc complex was easier reduced than the other two complexes.

In comparison with the azpy and azpym complexes (Table 14), the $Ru(azpym)_2Cl_2$ showed the first reduction couple in the range –0.40 to –0.48 V, while the *ctc*-$[Ru(azpy)_2Cl_2]$ was exhibited at –0.85 V [Leesakul, N., 2000]. Thus, the azpym complexes displayed the highest potential in this family. The π-acidity order of the ligands are as follows:

$$azpy < azine < azpym$$

Table 14. Cyclic voltammetric data of the azine, azpy, azpym and its complexes in acetonitrile

Compounds	Reduction potentials (V)
azine	-1.28
$[Ru(azine)_2Cl_2]$	-0.59 to -0.72
azpy	-1.61
ctc-$[Ru(azpy)_2Cl_2]$	-0.85
azpym	-1.14
$[Ru(azpym)_2Cl_2]$	-0.40 to -0.48

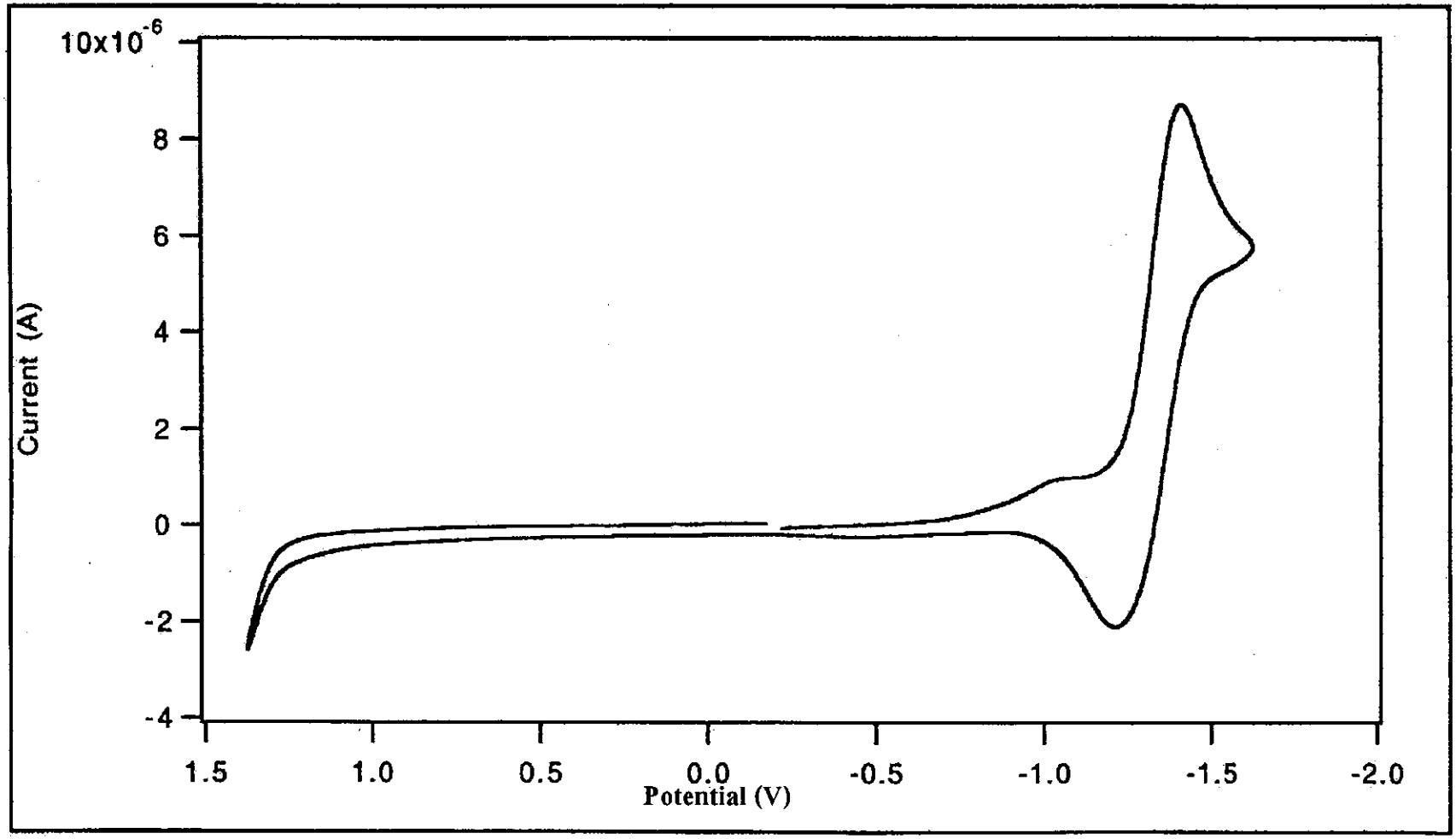

Figure 35. Cyclic voltammogram of azine in 0.1 M TBAH CH_3CN at scan rate 50 mV/s.

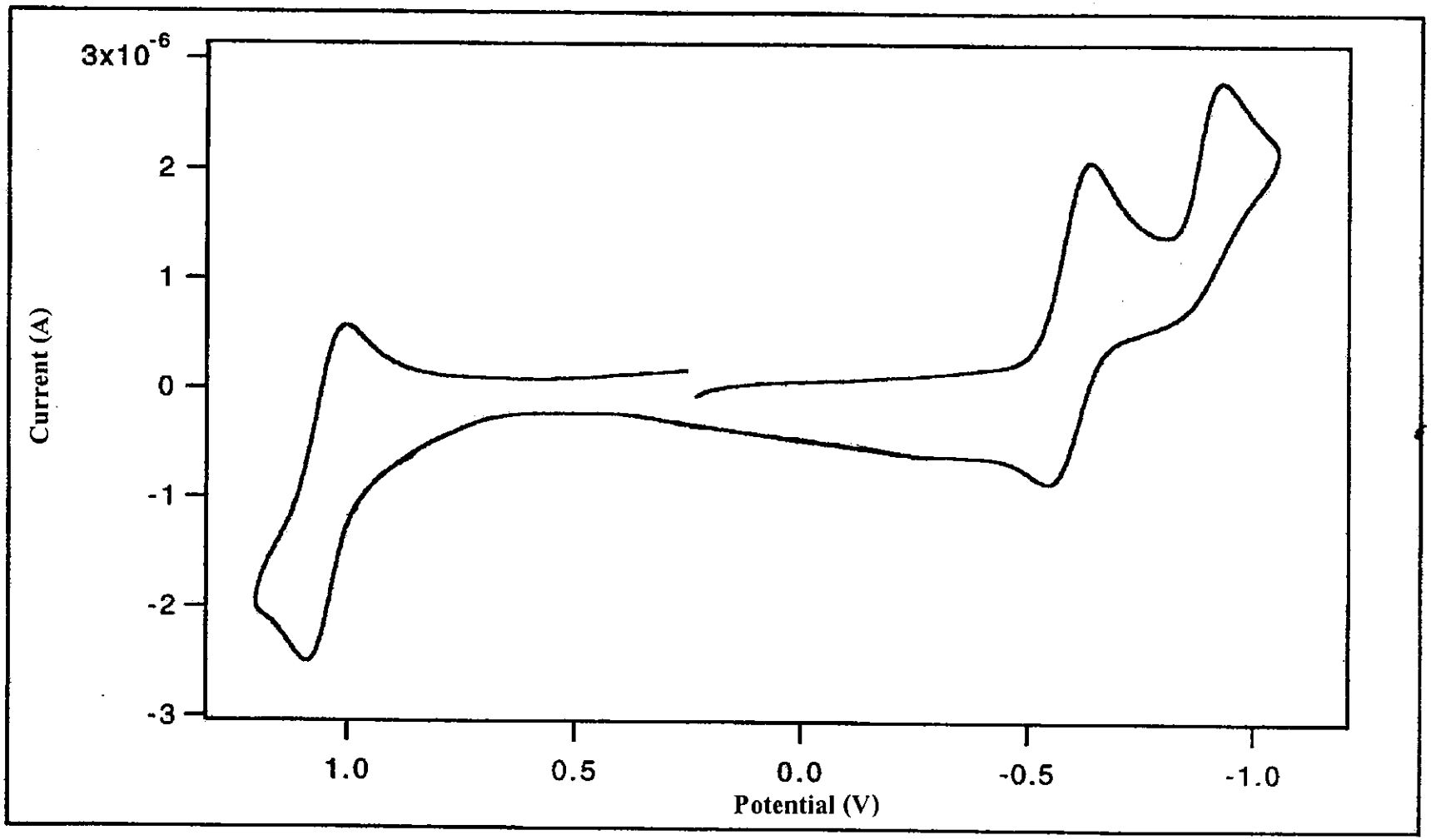

Figure 36. Cyclic voltammogram of *ctc*-[Ru(azine)$_2$Cl$_2$] in 0.1 M TBAH CH_3CN at scan rate 50 mV/s.

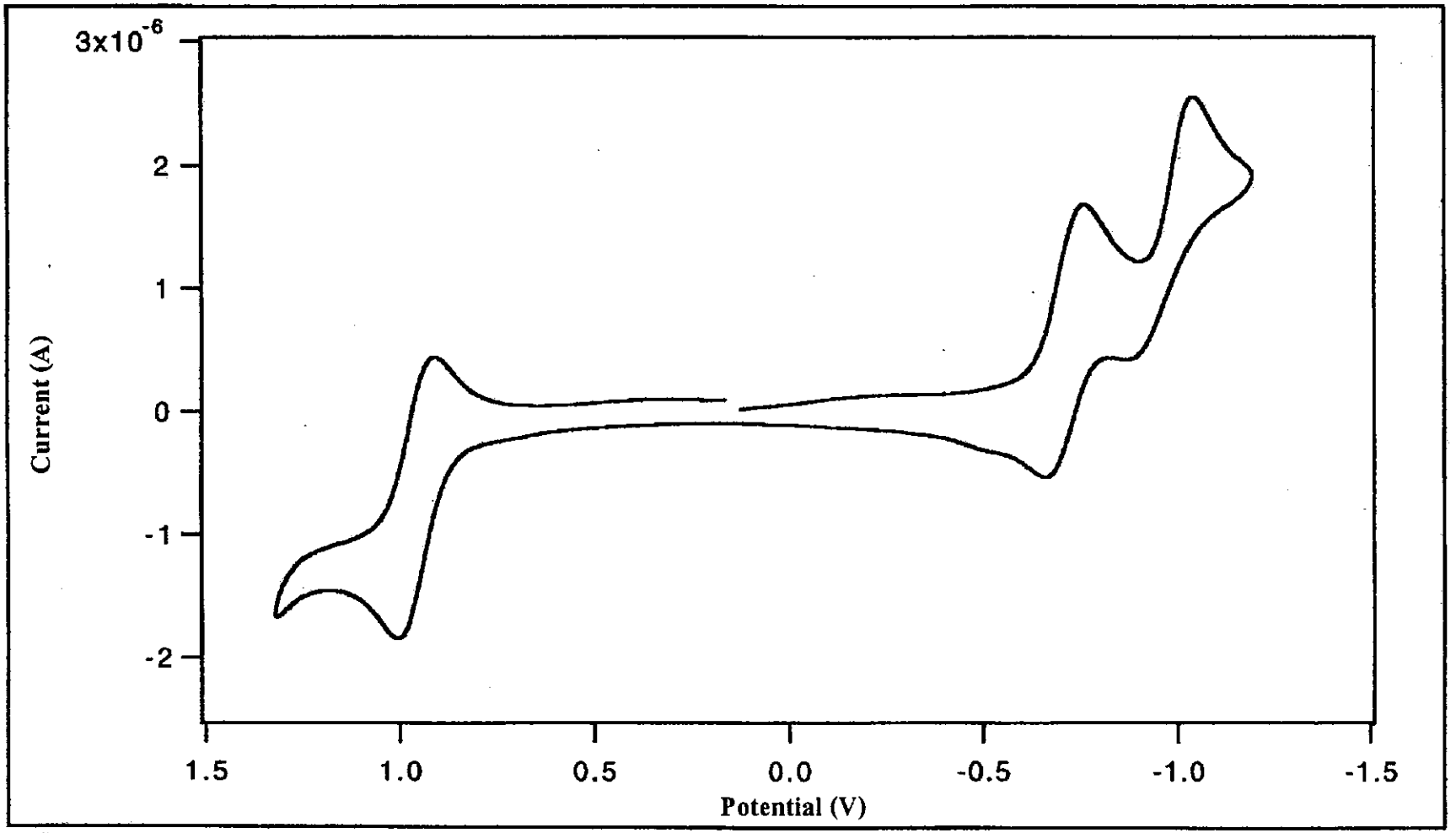

Figure 37. Cyclic voltammogram of *ccc*-[Ru(azine)$_2$Cl$_2$] in 0.1 M TBAH CH_3CN at scan rate 50 mV/s.

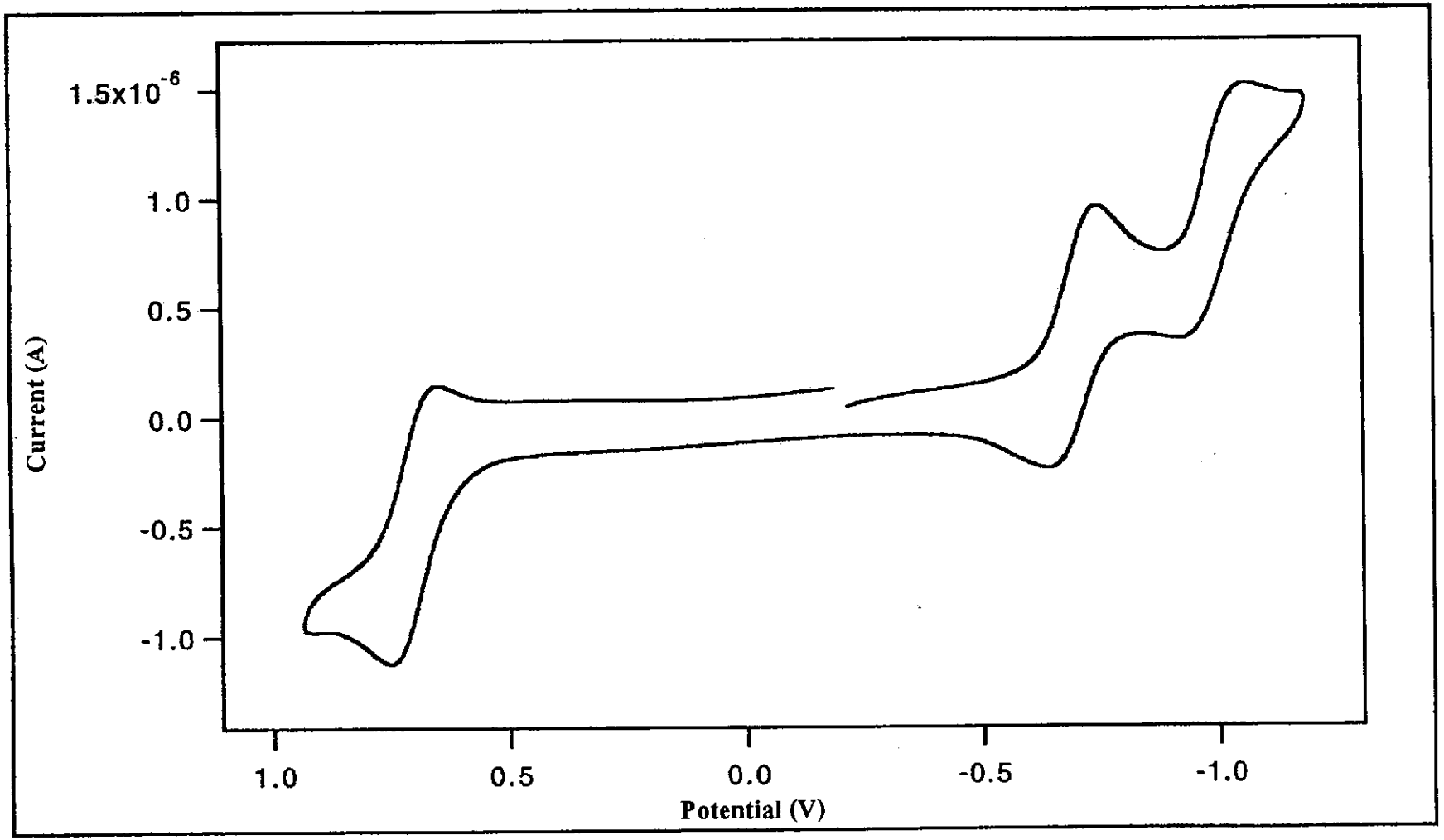

Figure 38. Cyclic voltammogram of *tcc*-[Ru(azine)$_2$Cl$_2$] in 0.1 M TBAH CH_3CN at scan rate 50 mV/s.

3.2.7 X-ray Crystallography

The X-ray crystallography is the most important technique to identify the geometry of compound. The single crystals of both *ctc*-[Ru(azine)$_2$Cl$_2$] and *tcc*-[Ru(azine)$_2$Cl$_2$] were grown by slow evaporation of toluene-dichloromethane solutions of the complexes. The structures of the two complexes showed six coordination around the ruthenium atom.

X-ray structure of *ctc*-[Ru(azine)$_2$Cl$_2$]

The crystal structure of ctc complexes is shown in Figure 40. The crystallgraphic data are shown in Table 15. Selected bond parameters associated with the metal ions are listed in Table 16.

Table 15. Crystallographic data of the *ctc*-[Ru(azine)$_2$Cl$_2$] complex

Empirical formula	$C_{21}H_{18}Cl_4N_8Ru$
Formula weight	625.30
Temperature	293(2) K
Wavelength	0.71073 Å
Crystal system	Monoclinic
Space group	P2(1)/c
Unit cell dimensions	a = 7.6447(4) Å $\alpha = 90^\circ$
	b = 17.9118(10) Å $\beta = 95.5250(10)^\circ$
	c = 18.5622(11) Å $\gamma = 90^\circ$
Volume	2529.9(2) Å ^{3}

Table 15. (continued)

Z	4
Density (calculated)	1.642 mg/m^3
Absorption coefficient	1.069 mm^{-1}
Goodness-of-fit on F^2	1.067
Final R indices [I>2sigma(I)]	R1 = 0.0399, wR2 = 0.0963
R indices (all data)	R1 = 0.0487, wR2 = 0.1008

Table 16. Selected bond lengths (Å) and angles (°) for *ctc*-[Ru(azine)$_2$Cl$_2$] complex

Ru(1)-N(8)	1.971(2)	Ru(1)-N(1)	2.019(2)
Ru(1)-N(4)	1.990(2)	Ru(1)-N(5)	2.019(2)
Ru(1)-Cl(1)	2.4007(8)	Ru(1)-Cl(2)	2.383(8)
N(3)-N(4)	1.289(3)	N(7)-N(8)	1.297(3)
N(8)-Ru(1)-N(4)	101.50(10)	N(4)-Ru(1)-Cl(2)	169.98(7)
N(8)-Ru(1)-N(5)	77.24(10)	N(5)-Ru(1)-Cl(2)	86.76(7)
N(4)-Ru(1)-N(5)	102.24(10)	N(1)-Ru(1)-Cl(2)	94.31(7)
N(8)-Ru(1)-N(1)	99.34(10)	N(8)-Ru(1)-Cl(1)	170.21(7)
N(4)-Ru(1)-N(1)	76.99(10)	N(4)-Ru(1)-Cl(1)	85.33(7)
N(5)-Ru(1)-N(1)	176.32(10)	N(5)-Ru(1)-Cl(1)	94.55(7)
N(8)-Ru(1)-Cl(2)	84.66(7)	N(1)-Ru(1)-Cl(1)	88.98(7)
Cl(2)-Ru(1)-Cl(1)	89.60(3)		

The atomic arrangement in the ctc complex involves sequentially two cis chlorine, trans-pyrazine and cis-azo and corresponds to the cis-trans-cis configuration. The coordination around the ruthenium atom is distorted octahedral. Moreover, there is the one molecule of CH_2Cl_2 solvent in the crystal structure as well.

The chelate bite angles extended by the two azine molecules were 77.24(10)° and 76.99(10) °. The cis-chloro angle of 89.60(3)° is very nearly the ideal octahedral angle and is comparable to the reported values (Santra, *et al.*, 1999).

The Ru(II)-N(azo) (N(4), N(8)) bond lengths (average, 1.981 Å) are shorter than the Ru(II)-N(pyrazine) (N(1), N(5)) bond lengths (average, 2.019 Å) by ~ 0.04 Å. The shortening may be due to greater π- backbonding, d(Ru)⟶ π*(azo). The N-N distance is not available for this free ligand: however, the data available in some free azo ligands suggest that it is ca. 1.25 Å (Santra, *et al.*, 1999). In the ctc complex, the average N-N distance is 1.293 Å. The coordination can lead to a decrease in the N-N bond order due to both the σ-donor and π-acceptor character of the ligands, with the latter character having a more pronounced effect, which may be the reason for elongation (supported by spectral data).

In comparison with the ctc-azpy complex [Seal, A., 1984], the Ru(II)-N (azo) bond lengths (average, 1.981 Å) are close to the bond distance in ctc-azine complex. While, the N-N distances in azpy complex (average 1.281 Å) are shorter than that in the azine complex (1.293(3) Å) by 0.012 Å. This indicated the π-back bonding power in the azopyrazines were greater than the azopyridine.

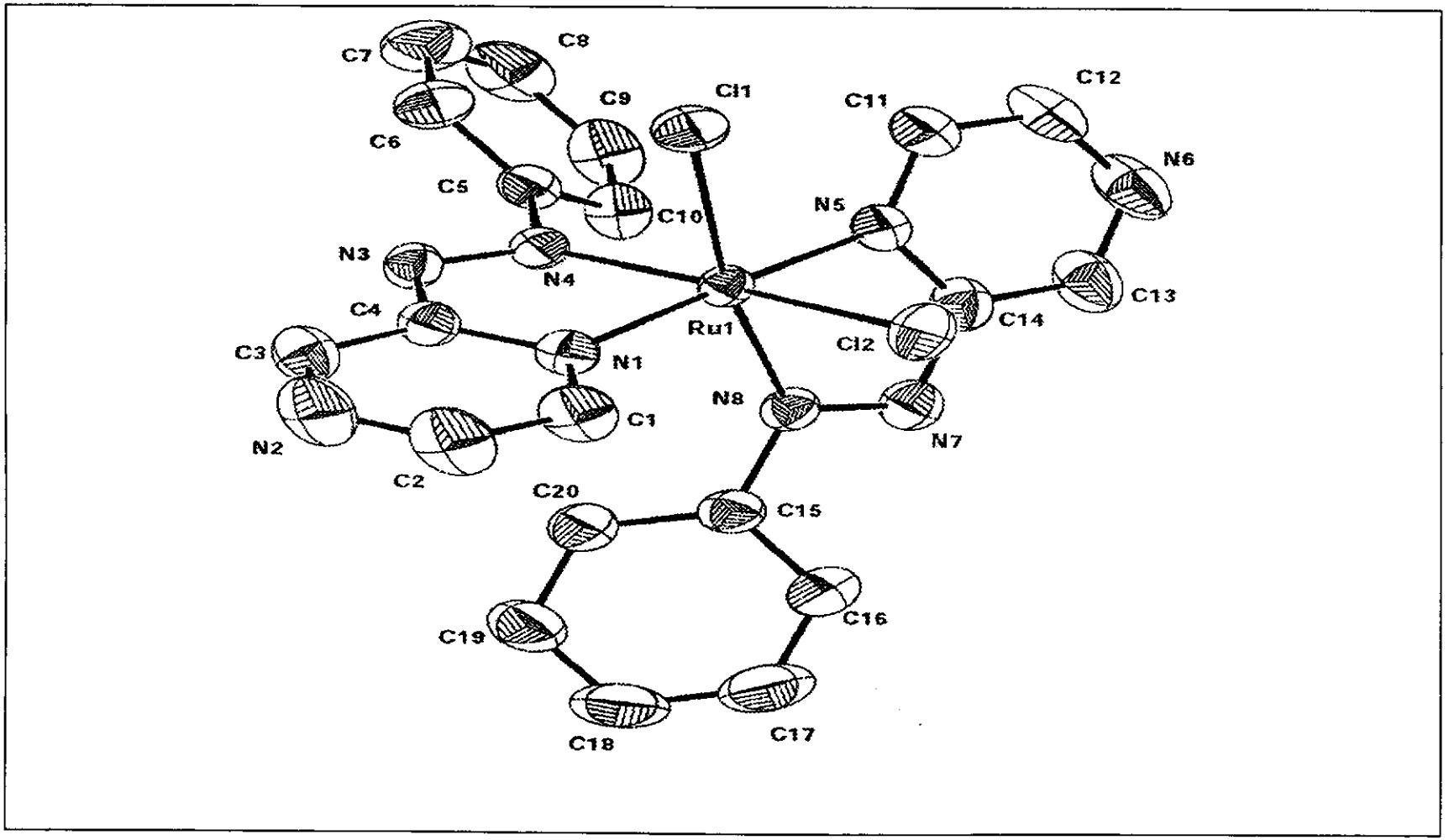

Figure 39. The structure of *ctc*-[Ru(azine)$_2$Cl$_2$] (H-atom omitted).

X-ray structure of *tcc*-[Ru(azine)$_2$Cl$_2$]

The crystal structure of tcc complex is shown in Figure 41. The crystallgraphic data are shown in Table 17. Selected bond parameters associated with the metal ions are listed in Table 18.

Table 17. Crystallographic data of the *tcc*-[Ru(azine)$_2$Cl$_2$] complex

Empirical formula	$C_{20}H_{16}Cl_2N_8Ru$
Formula weight	540.38
Temperature	293(2) K
Wavelength	0.71073 Å
Crystal system	Triclinic
Space group	P-1
Unit cell dimensions	a = 6.9893(5) Å α = 73.3200(10)°
	b = 11.6506(8) Å β = 88.8780(10)°
	c = 13.4254(9) Å γ = 81.1570(10)°
Volume	1034.43(12) Å^3
Z	2
Density (calculated)	1.735 mg/m^3
Absorption coefficient	1.043 mm^{-1}
Max. and min. transmission	0.930 and 0.844
Goodness-of-fit on F^2	1.067
Final R indices [I>2sigma(I)]	R1 = 0.0291, wR2 = 0.0663
R indices (all data)	R1 = 0.0336, wR2 = 0.0683

Table 18. Selected bond lengths (Å) and angles (°) for *tcc*-[Ru(azine)$_2$Cl$_2$] complex

Ru-N(4)	1.9904(18)	Ru-N(8)	2.0097(18)
Ru-N(1)	2.0935(18)	Ru-N(5)	2.0941(19)
Ru-Cl(2)	2.3609(6)	Ru-Cl(1)	2.3836(6)
N(8)-N(7)	1.284(3)	N(4)-N(3)	1.290(3)
N(4)-Ru-N(8)	104.18(7)	N(1)-Ru-Cl(2)	89.77(5)
N(4)-Ru-N(1)	75.89(7)	N(5)-Ru-Cl(2)	82.27(5)
N(8)-Ru-N(1)	173.03(7)	N(4)-Ru-Cl(1)	97.26(6)
N(4)-Ru-N(5)	172.29(7)	N(8)-Ru-Cl(1)	88.92(6)
N(8)-Ru-N(5)	75.40(7)	N(1)-Ru-Cl(1)	84.17(5)
N(1)-Ru-N(5)	105.49(7)	N(5)-Ru-Cl(1)	90.43(5)
N(4)-Ru-Cl(2)	90.18(6)	Cl(2)-Ru-Cl(1)	168.96(2)
N(8)-Ru-Cl(2)	97.19(6)		

In the tcc complex, the two chloride atoms occupy the trans positions. The two azine ligands bind the ruthenium ion through two pyrazine-N and two azo-N atoms and correspond to the trans-cis-cis configuration. The coordination geometry of the ruthenium(II) was distorted octahedral.

The Cl-Ru-Cl angle is 168.96(2) °, which is less than the ideal value of 180°. The chelate bite angle of the N(4)-Ru-N(1) is (75.89(7) °) close to the N(8)-Ru-N(5) bite angle (75.40(7) °).

The average N-N distance (1.287 Å) is slightly shorter than that in the ctc complex (1.293 Å). The Ru(II)-N(pyrazine) distances (average, 2.094 Å) are longer than those of Ru(II)-N(azo) (average, 2.000 Å) and this is an indication of an metal-ligand π-interaction that is localized in the metal-azo fragment. Furthermore, the

average N-N bond length in the tcc azpym complex (1.299(5) Å) [Santra, *et al.*, 1999] is longer than the tcc azine complex. According to the experiment, the π-back bonding in the azpym ligand were better than the azine ligand.

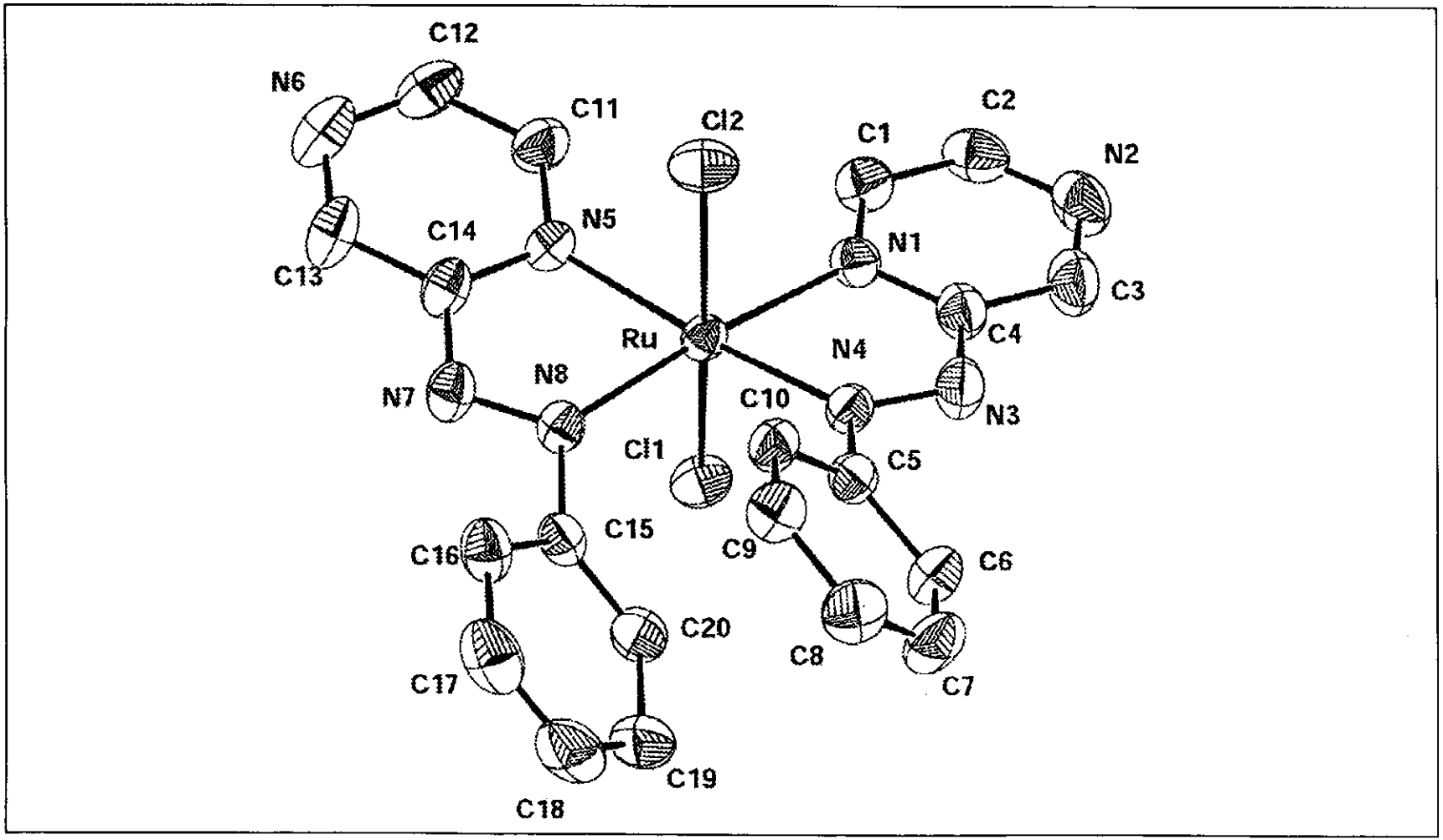

Figure 40. The structure of *tcc*-[Ru(azine)$_2$Cl$_2$] (H-atom omitted).